AD_____

Award Number: DAMD17-01-1-0806

TITLE: Bone Geometry as a Predictor of Tissue Fragility and Stress Fracture Risk

PRINCIPAL INVESTIGATOR: Karl J. Jepsen, Ph.D.

CONTRACTING ORGANIZATION: Mount Sinai School of Medicine
New York, NY 10029-6574

REPORT DATE: October 2005

TYPE OF REPORT: Annual

PREPARED FOR: U.S. Army Medical Research and Materiel Command
Fort Detrick, Maryland 21702-5012

REPORT DOCUMENTATION PAGE

Form Approved
OMB No. 0704-0188

1. REPORT DATE *(DD-MM-YYYY)*	**2. REPORT TYPE**	**3. DATES COVERED** *(From - To)*
01-10-2005	Annual	10 Sep 2004 – 10 Sep 2005

4. TITLE AND SUBTITLE
Bone Geometry as a Predictor of Tissue Fragility and Stress Fracture Risk

5a. CONTRACT NUMBER

5b. GRANT NUMBER
DAMD17-01-1-0806

5c. PROGRAM ELEMENT NUMBER

6. AUTHOR(S)
Karl J. Jepsen, Ph.D.

E-mail: karl.jepsen@mssm.edu

5d. PROJECT NUMBER

5e. TASK NUMBER

5f. WORK UNIT NUMBER

7. PERFORMING ORGANIZATION NAME(S) AND ADDRESS(ES)

Mount Sinai School of Medicine
New York, NY 10029-6574

8. PERFORMING ORGANIZATION REPORT NUMBER

9. SPONSORING / MONITORING AGENCY NAME(S) AND ADDRESS(ES)
U.S. Army Medical Research and Materiel Command
Fort Detrick, Maryland 21702-5012

10. SPONSOR/MONITOR'S ACRONYM(S)

11. SPONSOR/MONITOR'S REPORT NUMBER(S)

12. DISTRIBUTION / AVAILABILITY STATEMENT
Approved for Public Release; Distribution Unlimited

13. SUPPLEMENTARY NOTES

14. ABSTRACT
Having a narrow tibia relative to body mass has been shown to be a major predictor of stress fracture risk and fragility. The reason for this phenomenon is not understood. Based on studies of genetically distinct inbred mouse strains, we found a reciprocal relationship between bone mass and bone quality, such that slender bones are associated with more damageable bone tissue. We postulate that a similar reciprocal relationship between bone mass and bone material properties exists in the human skeleton. The intriguing possibility that slender bones, like those we have demonstrated in animal models, may be composed of more damageable material than larger bones has not been considered. To test this hypothesis, we propose to determine whether whole bone geometry is a predictor of tissue fragility in the tibia from young male donors. Tissue damageability will be assessed from biomechanical testing of compact bone samples and correlated with measures of bone slenderness. Specimens will be subjected to detailed analyses of bone microstructure, composition, and microdamage content. In the second set of experiments, these analyses will be repeated for female donors to test for gender differences in tissue fragility. Further, we will test whether fragility in cortical bone is a predictor of fragility in cancellous bone. Finally, we will conduct ultrasound measurements to identify an ultrasound parameter that is sensitive to the presence of damage and could be used for early diagnosis of stress fractures.

15. SUBJECT TERMS
Stress fracture, Bone Mass, Bone Quality, Biomechanics, Damage, Fatigue, Ultrasound. Non-Invasive measures. Genetic background

16. SECURITY CLASSIFICATION OF:			**17. LIMITATION OF ABSTRACT**	**18. NUMBER OF PAGES**	**19a. NAME OF RESPONSIBLE PERSON**
					USAMRMC
a. REPORT	**b. ABSTRACT**	**c. THIS PAGE**			**19b. TELEPHONE NUMBER** *(include area code)*
U	U	U	UU	26	

Standard Form 298 (Rev. 8-98)
Prescribed by ANSI Std. Z39.18

Table of Contents

Introduction

Having a narrow tibia relative to body mass has been shown to be a major predictor of stress fracture risk and fragility (Giladi et al, 1987; Milgrom et al, 1989; Beck et al, 1996). The reason for this phenomenon is not understood. Based on studies of genetically distinct inbred mouse strains, we found a reciprocal relationship between bone mass and bone quality, such that slender bones are associated with more damageable bone tissue (Jepsen et al, 2001). *We postulate that a similar reciprocal relationship between bone mass and bone material properties exists in the human skeleton. The intriguing possibility that slender bones, like those we have demonstrated in animal models, may be composed of more damageable material than larger bones has not been considered.* To test this hypothesis, we propose to determine whether whole bone geometry is a predictor of tissue fragility in the tibiae from young male donors. Tissue damageability will be assessed from biomechanical testing of compact bone samples and correlated with measures of bone slenderness. Specimens will be subjected to detailed analyses of bone microstructure, composition, and microdamage content. In the second set of experiments, these analyses will be repeated for female donors to test for gender differences in tissue fragility.

Body

In the fourth year of this grant, we focused on continuing the tissue-level mechanical tests for the female bones and the histological analysis of the male bones. We applied for a no-cost extension to continue this research in order to finish the last half dozen female samples. Obtaining human samples from females ages 18-40 has been a challenge recently and we have expanded our resources to include the Anatomy Gifts Registry and the National Disease Research Interchange.

In year three, we had begun a series of experiments that examined whether ultrasound has the sensitivity to detect the presence of damage in bone. Most studies have found that ultrasound is insensitive to damage. We have found that damage affects the viscoelastic properties of bone to a greater degree than the stiffness properties and we have focused our attention on the attenuation of the ultrasound signal as this may be more sensitive to the presence of damage. A student for the City University of New York worked on this project and found that, like prior work, the velocity of the ultrasound signal was insensitive to the presence of damage. He examined the attenuation (a measure related to the viscoelastic properties of bone) following damage accumulation, however, could not make a reasonable conclusion because of difficulties in matching the size of the sample to the size of the ultrasound transducer. Although viscous properties may be more sensitive to the presence of damage, we concluded from this study that it was not practical to reliably measure this parameter using machined bone samples from human tibiae. We would have to develop protocols using a larger animal (e.g., cow) to further test this.

A major outcome of this grant was finding that tissue-level mechanical properties vary with the size of the tibia (Tomassini et al, JBMR, 2005). Tissue modulus decreased with bone size, whereas post-yield strain and total energy increased with bone size. Not all of these correlations were significant indicating that the relationship between bone morphology and tissue level mechanical properties was subtle. The damage parameter decreased with bone size but only when the morphological properties were normalized for body weight and size. These results indicated that smaller bones are comprised of tissue that is more stiff and less ductile (i.e., more brittle) compared to larger bones. In year four, we conducted a histological evaluation to determine if we could explain the variability in tissue-level mechanical properties based on differences in tissue microstructure. The mid-span region of the samples that were subjected to damage accumulation tests were stained with basic fuchsin and embedded, undecalcified, in poly-methylmethacrylate. Transverse sections (150micron thickness) were cut using a low-speed diamond waffering saw, ground and polished to 100micron thickness, and mounted on glass slides for evaluation. Digitial images of each cross-section were analyzed for the area fraction of Haverisian porosity, the area fraction of non-Haverisian porosity, the total porosity, the area fraction occupied by full osteons, the area fraction occupied by osteon fragments, and the area fraction occupied

by circumferential (unremodeled) bone. Further, an adjacent portion of the test samples were subjected to standard ashing methods in order to assess ash content. We corrected the microstructural and compositional values for age-effects by linear regression analysis and then constructed a correlation matrix. We found that the post-yield strain ($p<0.04$) and total energy ($p<0.06$) were positively correlated with the area fraction of full osteons. No other significant correlations were observed. This indicated that having a lower area fraction of osteons lead to a more brittle failure mode. No significant correlations were observed between ash content and any of the mechanical properties tested. This contrasts with the results for the mouse femurs which showed that variation in whole bone ductility was explained largely by ash content (Jepsen et al, Mamm Genome, 2004).

Figure 1. Correlation between a) post-yield strain and b) total energy and the area fraction of full osteons.

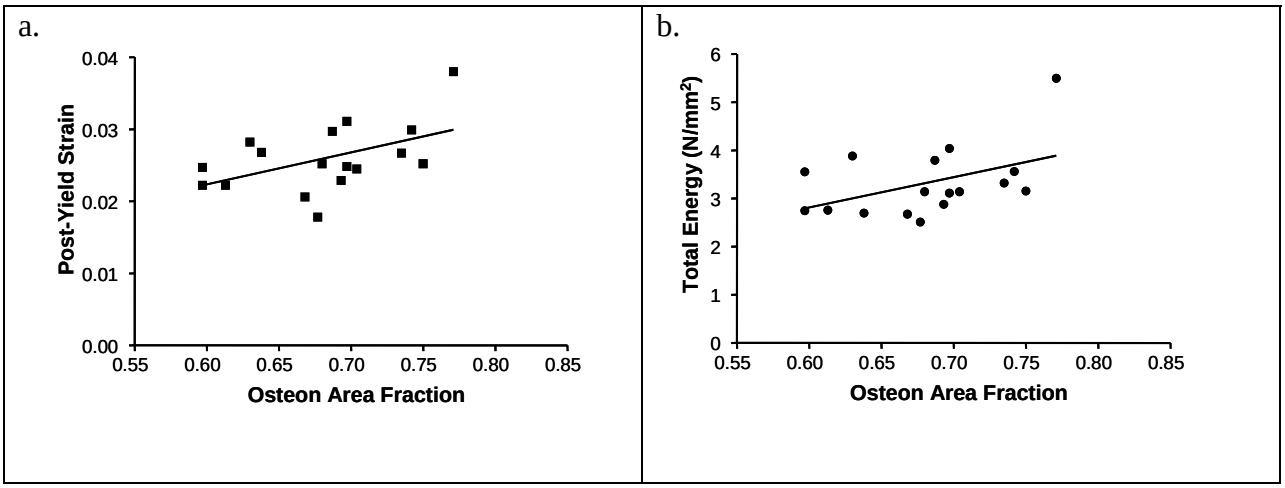

We have analyzed 12 of the 18 female tibia to date, and are aggressively trying to locate 6 more pairs of tibia. The problem with our current data set is that 11 of the 12 females range in age from 33-46. Consequently, the data set is not easily related to the males until we obtain additional samples in the 20-30 year old range. Obviously this is a challenge since this age group and gender is one of the rarest to find, particularly for samples that are free of bone-related illnesses. We are on the wait-list of several bone transplant organizations, and we anticipate that we should be able to secure the remaining 6 samples over the next year.

Key Research Accomplishments

The primary outcome of the grant thus far is that individuals with more slender bones appear to have different material properties. With increasing slenderness, the material is more stiff, less ductile, and more damageable. This supports are central hypothesis and may help explain why individuals with smaller tibiae are at higher risk of stress fractures.

Reportable Outcomes

Bouxien, ML, Jepsen KJ. Etiology and biomechanics of hip and vertebral fractures. *Atlas of Osteoporosis,* Second Edition. Current Medicine, Inc., Eds. Eric S. Orwoll, Stanley G. Korenman, 2003.

Jepsen K. The aging cortex: to crack or not to crack. *Osteoporos Int.* 2003 Sep;14 Suppl 5:57-66. 2003.

Tommasini SM, Nasser P, Jepsen KJ. Gender differences in bone slenderness are not related to material properties. Transactions Orthopaedic Research Society, 2002.

Tommasini SM, Morgan TG, van der Meulen MCH, Jepsen KJ. Genetic variation in vertebral mechanical properties determined by the relationship between morphological and compositional bone traits. Transactions Orthopaedic Research Society, 2003.

Jepsen KJ, Price C, Nadeau JH. Systems analysis of bone fragility. Pathways, Networks, and Systems: Theory and Experiments. Aegean Conference, 2003.

Tommasini SM, Nasser P, Jepsen KJ. The relationship between bone morphology and bone quality: Implications for stress fracture risk in young adult male tibiae. Poster and podium presentations as the American Society of Bone and Mineral Research Annual meeting, Seattle, WA, 2004.

Bird JE, Nasser P, Tommasini S, Casagrande D, Jepsen KJ. The relationship between continued periosteal apposition and bone fragility. Poster presentation at the American Society of Bone and Mineral Research Annual meeting, Seattle, WA, 2004.

Tommasini SM, Nasser P, Schaffler MB, Jepsen KJ. The relationship between bone morphology and bone quality in male tibiae: Implications for stress fracture risk. *Journal of Bone and Mineral Research*, 20(8):1372-1380, 2005.

Price C, Herman BC, Lufkin T, Goldman HM, Jepsen KJ. Genetic variation in bone growth patterns defines adult mouse bone fragility. *Journal of Bone and Mineral Research,* 20(11): 1983-1991, 2005.

Jepsen, KJ. *Assessing the mechanical properties of mineralized tissues. Invited talk,* Advances in Mineral Metabolism (AIMM); Snowmass, CO, 2005.

Jepsen, KJ. *Using mice to understand structure-function relationships in the skeleton.* Invited talk, Bone Quality Meeting; Sponsored by the National Institutes of Arthritis and Musculoskeletal and Skin Diseases (NIAMS) and the American Society of Bone and Mineral Research; Bethesda MD May 2-3, 2005.

Jepsen, KJ. *Biomechanical insights into the components of bone strength. Invited talk,* Alliance for Better Bone Health Sponsored Symposium at the Second Joint Meeting of the European Calcified Tissue Society (ECTS) and the International Bone and Mineral Society (IBMS), Geneva, Switzerland, June, 2005.

Jepsen, KJ. *Can heritable aspects of bone quality be enhanced through intervention? Invited talk,* American Society of Bone and Mineral Research; Working group on Bone Remodeling and Stress Fracture, Nashville, TN, 2005.

Funding

The data generated by this grant provided evidence that the mouse represents an important model for understanding the genetic variability in the human skeleton. This data helped secure an RO1 grant from the NIH (AR44927) titled, "Genetic Determination of Skeletal Fragility".

The data generated by this grant was also used in the submission of two NIH grants titled, “Genetic regulation of bone growth and development” and “Age-changes in bone morphology as a predictor of fracture risk”. The goal of the first grant is to identify chromosomes harboring quantitative trait loci influencing bone growth patterns. The goal of the second grant is to determine if 25 year changes in moment of inertia predict fracture incidence. This latter grant utilizes information from the Framingham Heart Study and was written in collaboration with the Boston University School of Public Health and the Hebrew Rehabilitation Center for the Aged.

Conclusions

The results to date have provided new insight into the relationship between bone morphology and tissue mechanical properties. The investigations of the mouse skeleton revealed that genetic variation in bone morphology strongly influence tissue mechanical properties through variations in matrix composition. The data suggest that a similar relationship may also exist in the human skeleton. Thus, individuals who have smaller (more narrow) tibia for their body size may compensate for the smaller geometry through variation in tissue-level mechanical properties. One of the side effects of this compensation is altered damageability which may be revealed under extreme physical activity such as that experience during military training.

References

Beck TJ, Ruff CB, Mourtada FA, Shaffer RA, Maxwell-Williams K, Kao GL, Sartoris DJ, Brodine S. Dual-energy X-ray absorptiometry derived structural geometry for stress fracture prediction in male U.S. Marine Corps recruits. *J Bone Miner Res,* 11:645-653, 1996.

Giladi M, Milgrom C, Simkin A, Stein M, Kashtan H, Margulies J, Rand N, Chisin R, Steinberg R, Aharonson Z, et al. Stress fractures and tibial bone width. A risk factor. *J Bone Jt Surg Br,* 69:326-329, 1987.

Jepsen, KJ, Pennington, DE, Lee, Y-L, Warman, M, Nadeau, J. Bone brittleness varies with genetic background in A/J and C57BL/6J inbred mice. *J Bone Miner Res,* 16(10):1854-1862, 2001.

Jepsen KJ, Akkus O, Majeska RJ, Nadeau JH. Hierarchical relationship between genetically determined bone traits and whole bone mechanical properties in inbred mice. *Mammalian Genome*, 14(2):97-104, 2003.

Milgrom C, Giladi M, Simkin A, Rand N, Kedem R, Kashtan H, Stein M, Gomori M. The area moment of inertia of the tibia: A risk factor for stress fractures. J Biomech 22:1243-1248, 1989.

Price C, Herman BC, Lufkin T, Goldman HM, Jepsen KJ. Genetic variation in bone growth patterns defines adult mouse bone fragility. *Journal of Bone and Mineral Research,* 20(11): 1983-1991, 2005.

Tommasini SM, Nasser P, Schaffler MB, Jepsen KJ. The relationship between bone morphology and bone quality in male tibiae: Implications for stress fracture risk. *Journal of Bone and Mineral Research,* 20(8):1372-1380, 2005.

Appendix 1

Tommasini SM, Nasser P, Schaffler MB, Jepsen KJ. The relationship between bone morphology and bone quality in male tibiae: Implications for stress fracture risk. *Journal of Bone and Mineral Research,* 20(8):1372-1380, 2005.

Appendix 2

Price C, Herman BC, Lufkin T, Goldman HM, Jepsen KJ. Genetic variation in bone growth patterns defines adult mouse bone fragility. *Journal of Bone and Mineral Research,* 20(11): 1983-1991, 2005.

JOURNAL OF BONE AND MINERAL RESEARCH
Volume 20, Number 8, 2005
Published online on March 28, 2005; doi: 10.1359/JBMR.050326

Relationship Between Bone Morphology and Bone Quality in Male Tibias: Implications for Stress Fracture Risk

Steven M Tommasini,[1] Philip Nasser,[2] Mitchell B Schaffler,[2] and Karl J Jepsen[2]

ABSTRACT: Biomechanical properties were assessed from the tibias of 17 adult males 17–46 years of age. Tissue-level mechanical properties varied with bone size. Narrower tibias were comprised of tissue that was more brittle and more prone to accumulating damage compared with tissue from wider tibias.

Introduction: A better understanding of the factors contributing to stress fractures is needed to identify new prevention strategies that will reduce fracture incidence. Having a narrow (i.e., more slender) tibia relative to body mass has been shown to be a major predictor of stress fracture risk and fragility in male military recruits and male athletes. The intriguing possibility that slender bones, like those shown in animal models, may be composed of more damageable material has not been considered in the human skeleton.
Materials and Methods: Polar moment of inertia, section modulus, and antero-posterior (AP) and medial-lateral (ML) widths were determined for tibial diaphyses from 17 male donors 17–46 years of age. A slenderness index was defined as the inverse ratio of the section modulus to tibia length and body weight. Eight prismatic cortical bone samples were generated from each tibia, and tissue-level mechanical properties including modulus, strength, total energy, postyield strain, and tissue damageability were measured by four-point bending from monotonic (n = 4/tibia) and damage accumulation (n = 4/tibia) test methods. Partial correlation coefficients were determined between each geometrical parameter and each tissue-level mechanical property while taking age into consideration.
Results: Significant correlations were observed between tibial morphology and the mechanical properties that characterized tissue brittleness and damageability. Positive correlations were observed between measures of bone size (AP width) and measures of tissue ductility (postyield strain, total energy), and negative correlations were observed between bone size (moment of inertia, section modulus) and tissue modulus.
Conclusions: The correlation analysis suggested that bone morphology could be used as a predictor of tissue fragility and stress fracture risk. The average mechanical properties of cortical tissue varied as a function of the overall size of the bone. Therefore, under extreme loading conditions (e.g., military training), variation in bone quality parameters related to damageability may be a contributing factor to the increased risk of stress fracture for individuals with more slender bones.
J Bone Miner Res 2005;20:1372–1380. Published online on March 28, 2005; doi: 10.1359/JBMR.050326

Key words: bone biomechanics, stress fracture, bone quality, bone morphology, strength, damage, brittleness

INTRODUCTION

Stress fractures are overuse injuries of bone that are common among elite runners and military recruits.[1–3] Before injury, affected bones are typically normal with no acute injury. Morbidity from stress fractures ranges from minor pain to serious lifetime disability for the individual.[4] Stress fractures have been reported in the ribs, hip, spine, and metatarsals,[3,5] but vigorous weight-bearing activities, such as running and jogging, commonly lead to stress fractures of the lower extremities, especially the tibia.[3] During basic training, 1–5% of U.S. male military recruits sustain a stress fracture.[2] However, this incidence is two to five times higher in female recruits.[6] Stress fractures lead to loss of manpower, valuable loss of training time, expense of medical care, and discharge of affected soldiers.[7] A better understanding of the factors contributing to stress fractures is needed to identify new prevention strategies that will reduce fracture incidence.

A number of risk factors for stress fracture have been identified including physical fitness, external hip rotation, body height and weight, age, race, gender, muscle mass, motivation, footwear, smoking, and family history of osteoporosis.[1,4,8–10] One of the best predictors of stress fracture risk is bone geometry. Specifically, having a narrow (i.e., more slender) tibia relative to body mass has been shown to

The authors have no conflict of interest.

[1]New York Center for Biomedical Engineering, CUNY Graduate School, Department of Biomedical Engineering, City College of New York, New York, New York, USA; [2]Leni & Peter W. May Department of Orthopaedics, Mount Sinai School of Medicine, New York, New York, USA.

be a major predictor of stress fracture risk and fragility in male military recruits[1,2,11] and male athletes.[12] A stress fracture is thought to be a consequence of transiently reduced tissue strength arising from increased resorptive activity (i.e., increased porosity) that acts to repair damage induced by vigorous physical activity.[13] Thus, stress fractures may be pronounced in individuals with more slender bones because smaller bone size is thought to lead to higher tissue-level stresses and thus increased damage accumulation.[1,2] However, this postulate is based on the assumption that all bones are constructed in equivalent manners, and the contribution of variable tissue-level mechanical properties to stress fracture incidence has not been explored.

An examination of inbred mouse strains may help explain why bone size is a risk factor for stress fractures in the human skeleton. A comparison of adult A/J and C57BL/6J inbred mouse strains revealed that the bone slenderness was inversely related to mineral content (as measured by ash content) and, by correlation, tissue modulus and strength.[14] Mineral content has been shown to be positively correlated with tissue stiffness and strength.[15] These results suggested that bone morphology and mineral content were coordinately regulated so whole bone stiffness appropriately matched the mechanical demands imposed by weight bearing. However, the downside of regulating mineral content to match bone size was that mineral content was also negatively correlated with tissue ductility.[14,15] We postulate that a similar reciprocal relationship between bone size and bone quality exists in the human skeleton. The intriguing possibility that slender bones, like those shown in animal models, may be composed of more damageable material has not yet been considered in the human skeleton.

The goal of this study was to determine whether tissue-level mechanical properties vary with bone size in the human skeleton. This was tested by assessing the biomechanical properties of tibias from young adult males. Understanding why bone morphology is a risk factor for stress fractures should lead to better identification of those at risk and, ultimately, to early diagnosis, treatment, and modification of training regimens.

MATERIALS AND METHODS

Sample population

Tibias of 17 male donors (15 white, 1 Hispanic, 1 black) 32.9 ± 10.4 years of age (range, 17–46 years) were acquired from the Musculoskeletal Transplant Foundation (Edison, NJ, USA). Donor body weight and height were obtained from the source. Only donors with no known skeletal pathology were included in the study. The tibias were freshly harvested, wrapped in wet gauze, and stored in plastic bags at –40°C.

Whole bone morphology

Tibia length (L) was measured as the average distance between the distal articular center (the middle of the talar trochlear facet) and the two proximal articular centers (medial and lateral condyles)[16] using a large-capacity slide caliper with an accuracy of ±2.54 mm (Mantex Precision; Haglöf, Madison, MS, USA). Tibia width was measured in the antero-posterior (AP) and medial-lateral (ML) directions at 10% intervals from 30–70% of the total tibia length using a 300-mm vernier caliper with an accuracy of ±0.02 mm (Fowler Company, Newton, MA, USA).

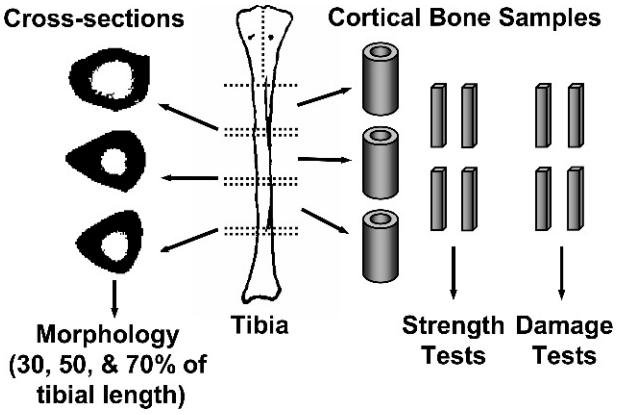

FIG. 1. Schematic of how whole tibias were sectioned to produce the 3-mm-thick sections used for cross-sectional morphology and cortical bone samples for biomechanical testing from three diaphyseal cylindrical sections (monotonic, $n = 4$/tibia; damage accumulation, $n = 4$/tibia).

Cross-sectional morphology was determined from 3-mm-thick middiaphyseal cross-sections cut at 30%, 50%, and 70% of the total tibia length (Fig. 1) using a diamond coated metallurgical saw (Model 660; South Bay Technology, San Clemente, CA, USA). A calibrated image of each cross-section was obtained using a digital camera at a 0.024 mm/pixel resolution. Image analysis software (IMAQ Vision Builder 6.0; National Instruments, Austin, TX, USA) was used to threshold each image and quantify cortical area (CtAr), the moments of inertia about the AP (I_{AP}) and ML (I_{ML}) axes, the polar moment of inertia ($J = I_{AP} + I_{ML}$), and the section modulus in the AP (J/APwidth/2) and ML (J/MLwidth/2) directions. Moment of inertia and section modulus were assessed because these geometric measures are related to the bending and torsional stiffness of intact tibias. A slenderness index (S) was calculated in the AP and ML directions as the ratio of the AP and ML section modulus values, respectively, to tibia length and body weight[17]:

$$S = 1/\{[J/(\text{width}/2)]/(L \times BW)\} \quad (1)$$

where L = tibia length (mm) and BW = body weight (kg). The section modulus has been shown to scale linearly with body mass.[17] The inverse ratio was used so that a tibia with a large slenderness value is one that is thinner or gracile for the weight and height of an individual. A small slenderness value reflects a stocky or robust tibia. All morphological traits were averaged over the three cross-sections for each tibia.

Bone sample generation

Cortical bone samples were prepared from the diaphysis of each tibia for biomechanical testing (Fig. 1). The three diaphyseal cylindrical sections were rough-cut into antero-

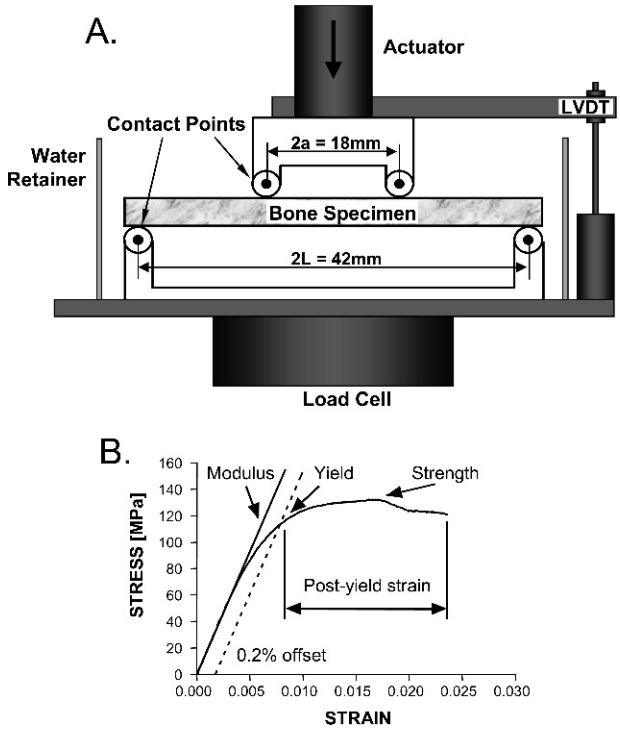

FIG. 2. (A) Schematic of the four-point bending device shows how cortical bone samples were tested. The span between the upper contact points is 2a = 18 mm, and the span between the lower contact points is 2L = 42 mm. (B) Typical stress-strain curve from the four-point bending monotonic tests shows how modulus, strength, postyield strain, and total energy were calculated.

lateral, antero-medial, and posterior regions. From each of these regions, one to three prismatic beams were cut using a diamond-coated metallurgical saw (Isomet; Buehler, Lake Bluff, IL, USA). The beams were machined to regular test samples using an automated CNC milling machine under constant irrigation (Modela MDX-20; Roland DGA, Irvine, CA, USA). Sample width (circumferential direction) was machined to 5 mm and length (longitudinal direction) was machined to 55 mm for all samples. Sample height (radial direction) was 2.5 mm except for four tibias with thin cortices, which were machined to 2.2 mm. A total of eight samples were generated from each tibia and randomly distributed to monotonic ($n = 4$) and damage accumulation ($n = 4$) test groups. All samples were stored at –40°C in gauze saturated with PBS with added calcium[18] and placed individually in airtight bags.

Monotonic failure properties

Tissue-level mechanical properties were assessed by loading four cortical bone samples from each tibia to failure in four-point bending at 0.05 mm/s (Fig. 2A) using a servohydraulic materials testing system (Instron model 8872; Instron, Canton, MA, USA). Specimens were submerged in a PBS solution with added calcium[18] and maintained at 37°C throughout all tests. Load and deflection were converted to stress and strain using the following equations, which take yielding into consideration[19]:

$$\sigma = 2[2M + \phi(dM/d\phi)]/bh^2 \quad (2)$$

$$\varepsilon = h\phi/2a = \tfrac{1}{2}h\Delta[(L - a)/(2a^3/3 - a^2L + L^3/3)] \quad (3)$$

where σ and ε are the stress and strain at the outer surface of the beam, M = applied moment, b = specimen width, h = specimen height, a = ½ the span between the upper two load points = 9 mm, L = ½ the span between the two lower load points = 21 mm, ϕ = angle of inclination = a/ρ, and $d/d\phi$ is the derivative with respect to ϕ. The angle of inclination was written in terms of the measured deflection (Δ) by estimating the curvature (ρ) using standard beam equations. Mechanical properties were calculated from the stress-strain curves, and these included modulus, strength, total energy, and postyield strain (Fig. 2B). Modulus was calculated from a linear regression of the initial portion of the stress-strain curve. Yield was determined using the 0.2% offset method. Postyield strain was defined as the strain at failure minus the strain at yield. All properties were averaged over the four samples tested for each tibia.

Damage accumulation tests

Tissue damageability was assessed using a protocol designed to induce and accumulate cracks in cortical bone specimens. The accumulation of damage leads to measurable degradation of mechanical properties.[20] Therefore, the degradation of mechanical properties can be used as an index of matrix damage. Four cortical bone samples from each tibia were subjected to a fifteen cycle damage accumulation protocol (Fig. 3A) similar to that described previously.[21] For this protocol, "diagnostic" cycles (1, 3, 5, 7, 9, 11, 13, and 15) were interposed between "damage" cycles (2, 4, 6, 8, 10, 12, and 14). For the diagnostic cycles, the specimens were loaded in four-point bending at 0.5 mm/s to 50% of the average displacement at yield (determined from the monotonic tests), held for 60 s, and unloaded at 0.5 mm/s. Preliminary studies indicated that this load level provided information on tissue-level mechanical properties without inducing additional damage. For the damage cycles, the specimens were loaded at 0.5 mm/s to 50%, 75%, 100%, 125%, 150%, 175%, and 200% of displacement at yield, respectively, held for 60 s, and unloaded at 0.5 mm/s. A 5-minute recovery period followed each damage cycle. Displacement at yield was used as a reference in the damage cycles because this parameter showed little variation among the test samples when subjected to monotonic four-point bending. The displacement at yield was 1.0 mm for the samples with a height of 2.5 mm and 1.07 mm for the samples with a height of 2.2 mm.

A mechanical measure of the amount of damage that accumulated within the test sample was quantified from the magnitude of stiffness degradation. For each diagnostic cycle, stiffness was calculated from a linear regression of the initial portion of the load-deformation curve. Specimen stiffness decreased nonuniformly with each cycle revealing increasing amounts of damage induced within each cycle and an overall damage accumulation by the end of the protocol (Fig. 3B). At the end of the test sequence, the overall

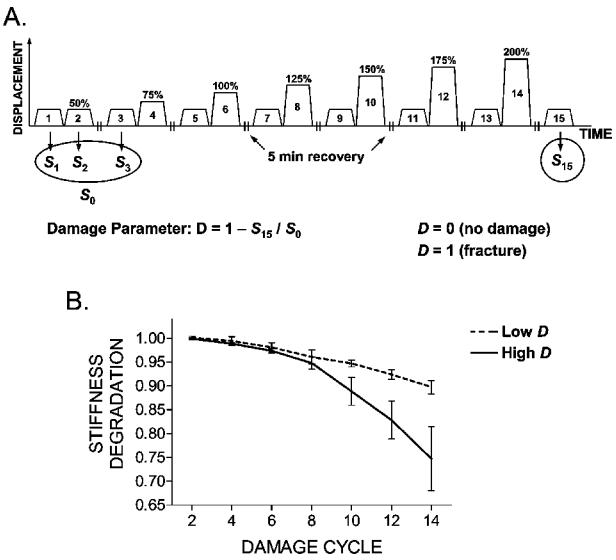

FIG. 3. (A) A 15-cycle loading protocol was used to induce damage within machined cortical bone specimens and to measure resultant stiffness degradation. Damage was induced during cycles 2, 4, 6, 8, 10, 12, and 14 by conducting relaxation tests at increasing levels of applied displacement (expressed as a percentage of the displacement at yield). Diagnostic cycles were interposed between damaging cycles. Each damage cycle was preceded by a diagnostic cycle at 50% of displacement at yield. A 5-minute recovery period was introduced after the damage cycles to relieve residual internal stresses. (B) The change in stiffness calculated between sequential diagnostic tests was plotted vs. cycle number for the damage tests. The dashed curve represents a specimen showing little stiffness degradation (i.e., little damage accumulation). The solid line represents a specimen showing large stiffness degradation (i.e., more damage accumulation).

damage parameter, D, was calculated by comparing the stiffness of the first and last diagnostic tests such that:

$$D = 1 - S_{15}/S_0, \quad (4)$$

where S_{15} is the stiffness of the last diagnostic cycle and S_0 is the average stiffness of the first two diagnostic cycles (S_1, S_3) and the first damage cycle (S_2).

Statistical analysis

All data were regressed against age using linear regression analysis to identify the properties that varied significantly with age (GraphPad Prism, San Diego, CA, USA). To determine whether bone morphology was related to tissue level material properties, partial correlation coefficients were determined between each geometrical parameter (e.g., I_{AP}, I_{ML}, J, S) and each tissue level mechanical property (modulus, strength, total energy, postyield strain, damageability) while taking age into consideration (Minitab, State College, PA, USA).[22]

RESULTS

The sample population showed broad ranges of body size, body stature, and bone morphology values (Table 1). Modulus and strength showed little variation among individuals (CV = 9.73% and 4.62%, respectively). However,

TABLE 1. VARIATION IN PROPERTIES AMONG YOUNG ADULT MALE TIBIAS

Property	*Mean ± SD*	*Range*
Age (years)	32.9 ± 10.4	17–46
Body weight (kg)	83.8 ± 25.1	57.2–158.8
Body height (cm)	177.7 ± 4.3	170.2–182.9
Body mass index (kg/m^2)	26.7 ± 8.0	17.1–51.7
Tibia length (cm)	38.1 ± 1.9	34.4–40.4
Cortical area (mm^2)	355.9 ± 55.2	268.3–511.1
AP width (mm)	31.2 ± 2.5	28.4–36.9
ML width (mm)	24.3 ± 2.3	19.9–30.6
AP moment of inertia (mm^4)	34,390 ± 10,149	19,466–60,698
ML moment of inertia (mm^4)	17,250 ± 5,945	8,246–34,734
Polar moment of inertia (mm^4)	51,640 ± 15,886	27,713–95,432
AP section modulus (mm^3)	3,279 ± 819	1,925–5,172
ML section modulus (mm^3)	4,188 ± 907	2,785–6,237
AP slenderness (1/mm^2/kg)	9.9 ± 2.0	6.5–13.4
ML slenderness (1/mm^2/kg)	7.7 ± 1.5	5.4–10.2
Modulus (GPa)	17.0 ± 1.7	13.4–19.0
Strength (MPa)	130.7 ± 6.1	120.8–144.5
Total energy (MPa)	3.3 ± 0.9	2.3–5.6
Post-yield strain	0.026 ± 0.006	0.016–0.039
Damage parameter (D)	0.165 ± 0.038	0.103–0.253

AP, antero-posterior direction; ML, medial-lateral direction.

postyield strain (CV = 24.0%), total energy (CV = 26.4%), and the damage parameter (CV = 23.0%) all showed large variability among the samples. Morphological measures such as AP width, section modulus, and the polar moment of inertia, J (Fig. 4), increased linearly with body weight ($R^2 = 0.59$, $p < 0.003$) and body mass index (BMI; $R^2 = 0.57$, $p < 0.004$), but were independent of body height ($R^2 = 0.01$, $p < 0.7$). These relationships did not change when the body weight values were corrected for age (data not shown). Body height was uncorrelated with body weight ($R^2 = 0.01$, $p < 0.8$), indicating that the sample population consisted of individuals with similar heights but widely varying body weights.

Significant age-related changes were observed for the tissue-level mechanical properties and the size of the tibia. A significant, positive correlation was observed between tibia slenderness in the AP ($R^2 = 0.31$, $p < 0.02$) and ML ($R^2 = 0.24$, $p < 0.05$) directions and age. However, I_{AP}, I_{ML}, and J did not vary with age, suggesting that the variation in slenderness with age was due largely to higher body weight and BMI ($R^2 = 0.29$–0.32, $p < 0.03$) values for the older individuals. Although tissue modulus did not vary significantly with age, tissue strength ($R^2 = 0.53$, $p < 0.001$), postyield strain ($R^2 = 0.44$, $p < 0.004$), and total energy ($R^2 = 0.32$, $p < 0.002$) were significantly lower for the older individuals. Furthermore, a significant, negative correlation was observed between the damage parameter and age ($R^2 = 0.41$, $p < 0.006$). This data suggested that, whereas the tibia became more slender relative to body size with age, the cortical tissue became progressively less strong and less ductile (i.e., more brittle) with age.

The correlation analysis showed significant correlations between tibial morphology and the mechanical properties that characterized tissue brittleness and damageability (Table 2). The relationships among tissue-level mechanical

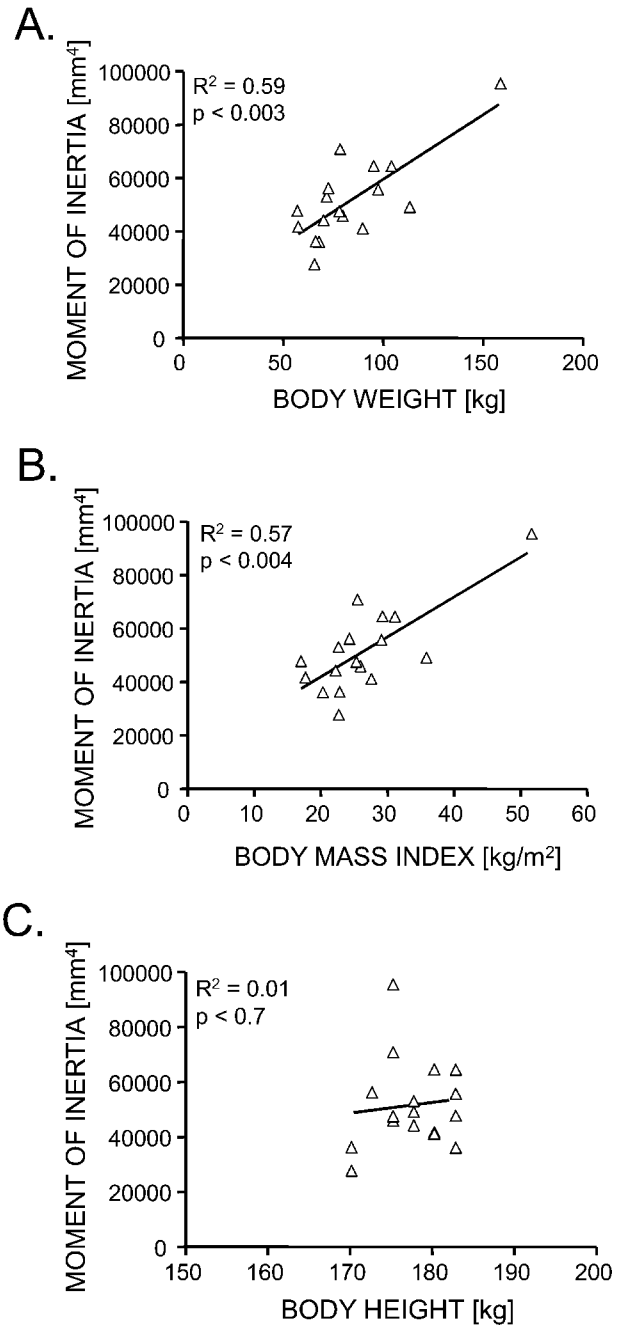

FIG. 4. The average cross-sectional polar moment of inertia of the tibia from males increased with (A) body weight and (B) body mass index but not with (C) body height. Removing the outlier changed the R^2 values to 0.24 ($p < 0.05$) for A and 0.20 ($p < 0.09$) for B.

properties and cross-sectional morphology were linear. Postyield strain and total energy increased significantly with AP width (Figs. 5A and 5B). Modulus decreased with I_{AP} ($p < 0.07$), J ($p < 0.08$), AP section modulus ($p < 0.05$), and ML section modulus (Figs. 5C–5F). Tissue damageability increased with tibia slenderness in the AP ($p < 0.05$; Fig. 6) and ML ($p < 0.09$) directions. These correlations, which were independent of age, indicated that a narrower bone was comprised of tissue that failed in a more brittle manner and accumulated more damage.

DISCUSSION

The results of this study revealed that the tissue-level mechanical properties of cortical bone varied with the size of the tibia. Positive correlations were observed between measures of bone size (AP width) and measures of tissue ductility (postyield strain, total energy), and negative correlations were observed between bone size (moment of inertia, section modulus) and tissue modulus. Many of these correlations were significant. The lack of significant correlation with all measures of bone size can be attributed largely to the complex shape of the tibia. The tibia has a triangular cross-section and, consequently, measures of width correlated significantly with mechanically relevant traits like cortical area and moment of inertia but explained only 50–80% of the variability in these measures (data not shown). These correlations would be greater if the cross-section had a circular shape. The variability in these correlations was sufficiently large that neither the linear (width) traits nor the integrated traits like area and moment of inertia correlated significantly with a particular tissue-level mechanical property simultaneously. Nevertheless, the data indicated that bones with smaller width were comprised of stiffer and less ductile (i.e., more brittle) material compared with larger, more robust bones. The correlation between tissue ductility and bone size may help explain why male military recruits[1,2,11] and male athletes[12] with narrow bones show a higher incidence of stress fractures compared with individuals with wide bones.

The development of the slenderness index[17] was for a "normal" range in height and weight and is probably not useful beyond this range. However, the morphological variation observed in our sample population was consistent with that reported for military recruits[1,2] and runners,[12] and height and weight were consistent with recent national averages.[23] As expected, bone size varied with body weight,[17] but did not vary with height (Fig. 4).[24] Thus, narrow bones came from less heavy individuals who were of similar height as those with wide tibias. Weight varied more than height for our sample population similar to that observed for the aged-matched national data. Furthermore, the variability in weight, specifically inclusion of one outlier (Fig. 4), did not affect the results (i.e., the heaviest person did not have an unusual slenderness value). Thus, the bones used in this study seem to be an appropriate size relative to body type.

The variation in long bone slenderness has been attributed to genetic and environmental factors influencing growth and development[25] and has been implicated as a risk factor for osteoporotic fracture.[26] To be relevant for military recruits, the sample population should have ranged in age between 18 and 25 years. However, for the age range in this study, the tissue-level mechanical properties varied linearly with age and were easily corrected using a linear regression method.[22] Consequently, the correlation analysis presented here provides relevant insight into the relationship observed between bone size and stress fracture risk

TABLE 2. PARTIAL CORRELATION COEFFICIENTS TAKING AGE INTO CONSIDERATION

	Modulus	*Strength*	*Total energy*	*PY strain*	*Damageability*
Cortical area	–0.24	0.03	0.37	0.40	–0.23
	(0.35)	(0.90)	(0.14)	(0.11)	(0.37)
AP width	–0.09	–0.03	**0.57**	**0.70**	–0.16
	(0.74)	(0.90)	**(0.02)**	**(0.002)**	(0.55)
ML width	–0.32	–0.22	0.34	0.41	–0.19
	(0.21)	(0.39)	(0.18)	(0.11)	(0.45)
AP moment of inertia	**–0.45**	–0.10	0.25	0.32	–0.27
	(0.07)	(0.70)	(0.34)	(0.21)	(0.29)
ML moment of inertia	–0.39	–0.18	0.22	0.28	–0.25
	(0.12)	(0.50)	(0.39)	(0.28)	(0.32)
Polar moment of inertia	**–0.43**	–0.13	0.24	0.31	–0.27
	(0.08)	(0.61)	(0.35)	(0.23)	(0.30)
AP section modulus	**–0.50**	–0.13	0.10	0.14	–0.30
	(0.04)	(0.62)	(0.70)	(0.60)	(0.25)
ML section modulus	**–0.47**	–0.05	0.18	0.23	–0.33
	(0.06)	(0.84)	(0.49)	(0.38)	(0.20)
Ap slenderness	0.36	0.10	0.09	0.03	**0.48**
	(0.15)	(0.69)	(0.72)	(0.92)	**(0.05)**
ML slenderness	0.23	–0.01	0.04	–0.05	0.41
	(0.39)	(0.96)	(0.89)	(0.84)	(0.10)

Pearson correlation coefficients are shown with p values in parentheses. Significant correlations are shown in bold. Abbreviations are as shown in Table 1.

for young adult males. Further studies are needed to determine if this relationship holds over a wider (older) age range.

The data provide a new paradigm that may explain how variation in bone slenderness contributes to stress fracture risk. Individuals with narrow tibias were previously thought to show increased fatigue damage during intense training because the smaller bone size would lead to an overload situation (i.e., higher tissue level stresses).[1,2,12] This interpretation was based on the assumption that tissue mechanical properties did not vary among individuals. However, the current results indicated that tissue-level mechanical properties do vary among individuals. Specifically, the data suggest that there are at least two important tissue-level mechanical property variations that need to be considered to understand why bone size is a risk factor for stress fractures. Narrower tibias were comprised of tissue that was more brittle (low total energy) and was prone to accumulate more damage compared with tissue from wider tibia. Having tissue that is more or less damageable may be inconsequential during day-to-day activities. However, tissue-level mechanical properties like total energy and ductility become particularly important in defining the response of bone to an extreme loading condition, such as that expected during military training or during a fall. Total energy defines the amount of energy required to break a bone (important during a fall) and ductility and damageability define the amount of damage accumulated under overload or repetitive loading (important during military training). Furthermore, tissue stresses would be expected to remain higher for narrow tibias loaded in bending or torsion. Moment of inertia is related to the external diameter raised to the fourth power. Because whole bone stiffness and strength are correlated with moment of inertia,[17,27] a bone with a large external diameter should also show large overall stiffness and strength values. However, the ~30% variation in tissue modulus (Table 1) did not fully compensate for the ~100% variation in the moment of inertia or the section modulus (Table 1).[27] Thus, in situ damage accumulation may elicit a biological response (remodeling) that, coupled with the higher tissue stresses, exacerbates the fatigue process.[13,28] Consequently, individuals with narrow tibia may be at higher risk of stress fractures because of higher in vivo tissue stresses (overloading) coupled with tissue that is more prone to accumulating damage.

The data may also help explain why age is another risk factor for stress fractures.[7,29] Bone strength, postyield strain, and total energy decreased over the 17- to 46-year-old age range. This was consistent with previous studies[30–32] and indicated that cortical bone becomes less ductile (i.e., more brittle) and weaker with age and that these changes began early in life. This age-related decline in strength and ductility is thought to be a result of increased mineralization and remodeling.[33,34] Thus, even in the young adult age range, the amount of damage accumulated under vigorous loading regimens would be expected to increase with age. This variation in tissue ductility may increase the susceptibility of stress fracture risk for recruits that enter into military training at an older age.

These results, and those of others, indicated that not all cortical tissue was constructed in the same manner. The mechanical properties of cortical tissue vary with age,[30–32,35] across species,[35] among bones of the same individual,[36] and among anatomical sites within the same bone.[37,38] Here we showed that the average mechanical properties of cortical tissue also varied as a function of the overall size of the bone. This coupling between bone morphology and tissue-level mechanical properties has been attributed to an adaptive response of bone.[14,35,39] In this study, smaller tibia bone size was coupled with an increase

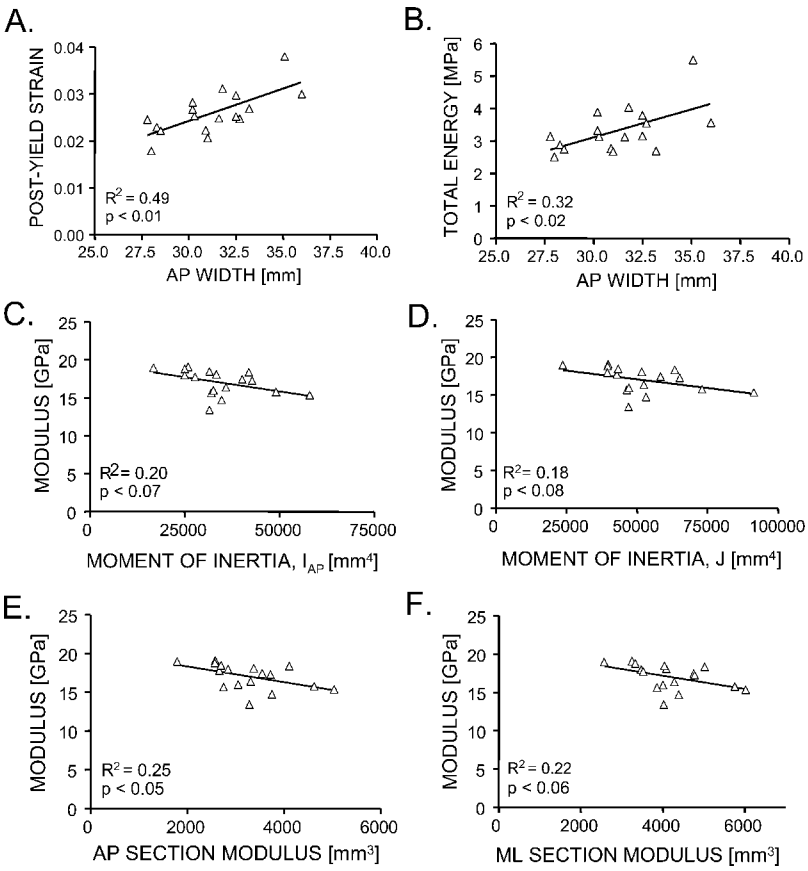

FIG. 5. (A) Postyield strain and (B) total energy correlated with AP width. Modulus decreased with (C) I_{AP}, (D) J, (E) AP section modulus, and (F) ML section modulus. Data were age-corrected based on a linear regression method.[22]

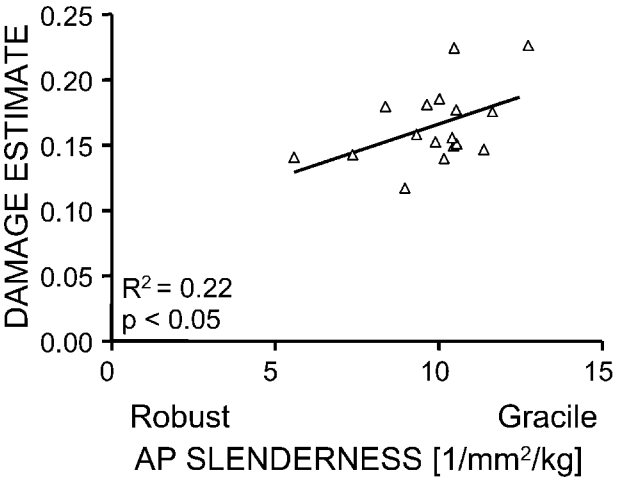

FIG. 6. Damageability correlated with AP slenderness suggesting that tibias that were more slender relative to body size and stature were comprised of tissue that accumulated more damage. Data were age-corrected based on a linear regression method.[22]

in tissue modulus. The goal of this adaptive response is to ensure that morphology and quality together meet mechanical demands. This coupling was observed when comparing bones subjected to widely varying mechanical demands from different species[35] and has also been used to explain the maturation of bone during growth.[40–43] Our current results suggested that this coupling might also exist for a particular bone (tibia) within the same species (human). Additional studies are needed to determine if similar relationships between morphology and quality exist for other long bones (femur, humerus, radius).

The relationship between morphology and tissue-level mechanical properties observed in the human skeleton was consistent with that observed for the mouse skeleton.[14] In both the mouse and human skeletons, genetic heterogeneity leads to variability in adult bone morphology and tissue level mechanical properties. A comparison of femurs from A/J and C57/BL6 (B6) inbred strains showed that A/J femurs were more slender than B6 as a result of the two strains having similar bone lengths, but A/J having a significantly smaller cross-sectional size and shape.[14] Despite the difference in bone size, the two strains showed similar whole bone stiffness values. The variability in bone slenderness was inversely related to mineral content, suggesting that bone morphology and mineral content were coordinately regulated so whole bone stiffness appropriately matched the mechanical demands imposed by weight bearing. However, as a result of regulating mineral content to match bone size, A/J femurs failed in a brittle manner and showed poor fatigue properties. In the human skeleton, smaller bones were stiffer and less ductile. Thus, a reciprocal relationship was observed between bone stiffness and ductility for both skeleton systems. This reciprocal relationship has been extensively reported for cortical bone,[15] and

it is thought to be a result of the nature of the compositional and structural factors that can be modulated on a biological level.[44–47] Although variation in mineral content may have explained the differences in brittleness for the mouse skeleton, we expect that the human skeleton will be more complex and that the variation in tissue-level mechanical properties will be a consequence of variable composition (mineral, collagen, water) as well as microarchitecture (lamellae, osteon size, porosity).

The calculated bending modulus and strength values, which were determined from machined bone samples and were thus quantified in a manner that was independent of bone size, were consistent with bone tensile properties,[30] as expected. Test samples were randomly selected to obtain representative mean values for each tibia and the variation in mechanical properties within each tibia was similar to the variability observed across tibias. Thus, we believe that the mean values reported here represent the generalized tissue-level mechanical behavior for each tibia.

Compared with back-calculating tissue-level mechanical properties from whole bone failure tests, the current method of measuring tissue-level mechanical properties directly from machined samples provided a broader range of mechanical properties that were needed to better understand why bone size is a risk factor for stress fractures. The mechanical properties included measures of ductility (i.e., postyield strain, total energy) as well as an independent measure of damageability (i.e., the damage parameter). These properties were chosen because they were relevant for understanding the material response of bones subjected to the vigorous, repetitive loading associated with military training and running. Postyield strain and total energy represent measures of tissue ductility and were assessed to discriminate between ductile and brittle failure modes. Materials that fail in a brittle manner show low postyield strain and total energy values. Variation in the ductility of cortical bone arises from differences in the initiation, accumulation, propagation, and coalescence of damage in the form of microcracks.[48,49] Variation in the damage parameter reflected differences in the amount of damage accumulated within the tissue and/or differences in the way damage degraded tissue stiffness. The damage parameter correlated negatively with postyield strain and total energy (R^2 = 0.22–0.25, $p < 0.05$) indicating that cortical tissue that failed in a brittle manner also tended to have higher tissue damageability or, accumulate more damage. Although the ex vivo bending tests do not necessarily reflect the in vivo loads imposed on the tibia,[17,50–52] the bending loads were expected to induce a combination of tensile, compressive, and shear damage[53] that may be sufficiently complex to represent a generalized variation in bone quality among human tibias.

The results of this study provide new insight into why bone size is a risk factor for stress fractures. Stress fractures are believed to be a consequence of excess damage accumulation following intense, repetitive activities. Biological processes that attempt to repair the damage may further weaken the tissue because the increased resorption results in increased tissue porosity.[54] However, the actual contribution of biological repair processes to stress fracture risk remains unclear.[55] Damage, in the form of microcracks, is the expected sequelae of repetitive loading following normal, daily activities.[56] Intense loading conditions, such as those associated with military training and long distance running, are expected to further increase in situ damage accumulation and degrade tissue-level mechanical properties.[13] Therefore, under extreme loading conditions (e.g., military training), variation in bone quality, specifically tissue damageability, may be a contributing factor to the increased risk of stress fracture for individuals with more slender bones. The current data suggested that bone morphology could be used as a predictor of tissue fragility and stress fracture risk in the absence of available noninvasive imaging techniques that accurately measure bone damageability.

ACKNOWLEDGMENTS

The authors thank the U.S. Department of Defense (DAMD17-01-1-0806; DAMD17-98-1-8515) and the Musculoskeletal Transplant Foundation for their support of this research.

REFERENCES

1. Milgrom C, Giladi M, Simkin A, Rand N, Kedem R, Kashtan H, Stein M, Gomori M 1989 The area moment of inertia of the tibia: A risk factor for stress fractures. J Biomech **22:**1243–1248.
2. Beck TJ, Ruff CB, Mourtada FA, Shaffer RA, Maxwell-Williams K, Kao GL, Sartoris DJ, Brodine S 1996 Dual-energy X-ray absorptiometry derived structural geometry for stress fracture prediction in male U.S. Marine Corps recruits. J Bone Miner Res **11:**645–653.
3. Milgrom C, Giladi M, Stein M, Kashtan H, Margulies JY, Chisin R, Steinberg R, Aharonson Z 1985 Stress fractures in military recruits. A prospective study showing an unusually high incidence. J Bone Joint Surg Br **67:**732–735.
4. Lappe JM, Stegman MR, Recker RR 2001 The impact of lifestyle factors on stress fractures in female Army recruits. Osteoporos Int **12:**35–42.
5. Milgrom C, Finestone A, Sharkey N, Hamel A, Mandes V, Burr D, Arndt A, Ekenman I 2002 Metatarsal strains are sufficient to cause fatigue fracture during cyclic overloading. Foot Ankle Int **23:**230–235.
6. Friedl KE, Nuovo JA, Patience TH, Dettori JR 1992 Factors associated with stress fracture in young army women: Indications for further research. Mil Med **157:**334–338.
7. Brudvig TJ, Gudger TD, Obermeyer L 1983 Stress fractures in 295 trainees: A one-year study of incidence as related to age, sex, and race. Mil Med **148:**666–667.
8. Bennell K, Matheson G, Meeuwisse W, Brukner P 1999 Risk factors for stress fractures. Sports Med **28:**91–122.
9. Jones BH, Thacker SB, Gilchrist J, Kimsey CD Jr, Sosin DM 2002 Prevention of lower extremity stress fractures in athletes and soldiers: A systematic review. Epidemiol Rev **24:**228–247.
10. Giladi M, Milgrom C, Simkin A, Danon Y 1991 Stress fractures. Identifiable risk factors. Am J Sports Med **19:**647–652.
11. Giladi M, Milgrom C, Simkin A, Stein M, Kashtan H, Margulies J, Rand N, Chisin R, Steinberg R, Aharonson Z 1987 Stress fractures and tibial bone width. A risk factor. J Bone Joint Surg Br **69:**326–329.
12. Crossley K, Bennell KL, Wrigley T, Oakes BW 1999 Ground reaction forces, bone characteristics, and tibial stress fracture in male runners. Med Sci Sports Exerc **31:**1088–1093.
13. Mori S, Burr DB 1993 Increased intracortical remodeling following fatigue damage. Bone **14:**103–109.

14. Jepsen KJ, Pennington DE, Lee YL, Warman M, Nadeau J 2001 Bone brittleness varies with genetic background in A/J and C57BL/6J inbred mice. J Bone Miner Res **16:**1854–1862.
15. Currey JD 1984 Effects of differences in mineralization on the mechanical properties of bone. Philos Trans R Soc Lond B Biol Sci **304:**509–518.
16. Ruff CB 2000 Body size, body shape, and long bone strength in modern humans. J Hum Evol **38:**269–290.
17. Selker F, Carter DR 1989 Scaling of long bone fracture strength with animal mass. J Biomech **22:**1175–1183.
18. Gustafson MB, Martin RB, Gibson V, Storms DH, Stover SM, Gibeling J, Griffin L 1996 Calcium buffering is required to maintain bone stiffness in saline solution. J Biomech **29:**1191–1194.
19. Nádai A 1950 Theory of Flow and Fracture of Solids. Engineering Societies Monographs. McGraw-Hill, New York, New York, USA.
20. Lemaitre J 1992 A Course on Damage Mechanics. Springer-Verlag, Berlin, New York.
21. Jepsen KJ, Davy DT 1997 Comparison of damage accumulation measures in human cortical bone. J Biomech **30:**891–894.
22. Di Masso RJ, Font MT, Capozza RF, Detarsio G, Sosa F, Ferretti JL 1997 Long-bone biomechanics in mice selected for body conformation. Bone **20:**539–545.
23. Ogden CL, Fryar CD, Carroll MD, Flegal KM 2004 Mean body weight, height, and body mass index, United States 1960-2002. Adv Data **347:**1–17.
24. Miller GJ, Purkey WW Jr 1980 The geometric properties of paired human tibiae. J Biomech **13:**1–8.
25. Christian JC, Yu PL, Slemenda CW, Johnston CC Jr 1989 Heritability of bone mass: A longitudinal study in aging male twins. Am J Hum Genet **44:**429–433.
26. Kiel DP, Hannan MT, Broe KE, Felson DT, Cupples LA 2001 Can metacarpal cortical area predict the occurrence of hip fracture in women and men over 3 decades of follow-up? Results from the Framingham Osteoporosis Study. J Bone Miner Res **16:**2260–2266.
27. van der Meulen MC, Jepsen KJ, Mikic B 2001 Understanding bone strength: Size isn't everything. Bone **29:**101–104.
28. Burr DB, Forwood MR, Fyhrie DP, Martin RB, Schaffler MB, Turner CH 1997 Bone microdamage and skeletal fragility in osteoporotic and stress fractures. J Bone Miner Res **12:**6–15.
29. Shaffer RA, Brodine SK, Almeida SA, Williams KM, Ronaghy S 1999 Use of simple measures of physical activity to predict stress fractures in young men undergoing a rigorous physical training program. Am J Epidemiol **149:**236–242.
30. Burstein AH, Reilly DT, Martens M 1976 Aging of bone tissue: Mechanical properties. J Bone Joint Surg Am **58:**82–86.
31. McCalden RW, McGeough JA, Barker MB, Court-Brown CM 1993 Age-related changes in the tensile properties of cortical bone. The relative importance of changes in porosity, mineralization, and microstructure. J Bone Joint Surg Am **75:**1193–1205.
32. Currey JD, Butler G 1975 The mechanical properties of bone tissue in children. J Bone Joint Surg Am **57:**810–814.
33. Evans FG 1976 Age changes in mechanical properties and histology of human compact bone. Yearb Phys Anthropol **20:**1361–1372.
34. Currey JD, Brear K, Zioupos P 1996 The effects of ageing and changes in mineral content in degrading the toughness of human femora. J Biomech **29:**257–260.
35. Currey JD 1979 Mechanical properties of bone tissues with greatly differing functions. J Biomech **12:**313–319.
36. Papadimitriou HM, Swartz SM, Kunz TH 1996 Ontogenetic and anatomic variation in mineralization of the wing skeleton of the Mexican free-tailed bat, *Tadarida brasiliensis*. J Zool **240:**411–426.
37. Riggs CM, Vaughan LC, Evans GP, Lanyon LE, Boyde A 1993 Mechanical implications of collagen fibre orientation in cortical bone of the equine radius. Anat Embryol (Berl) **187:**239–248.
38. Skedros JG, Dayton MR, Sybrowsky CL, Bloebaum RD, Bachus KN 2003 Are uniform regional safety factors an objective of adaptive modeling/remodeling in cortical bone? J Exp Biol **206:**2431–2439.
39. Ferretti JL, Capozza RF, Mondelo N, Zanchetta JR 1993 Interrelationships between densitometric, geometric, and mechanical properties of rat femora: Inferences concerning mechanical regulation of bone modeling. J Bone Miner Res **8:**1389–1396.
40. Ferretti JL, Cointry GR, Capozza RF, Frost HM 2003 Bone mass, bone strength, muscle-bone interactions, osteopenias and osteoporoses. Mech Ageing Dev **124:**269–279.
41. Heinrich RE 1999 Ontogenetic changes in mineralization and bone geometry in the femur of muskoxen (Ovibos moschatus). J Zool **247:**215–223.
42. Brear K, Currey JD, Pond CM 1990 Ontogenetic changes in the mechanical properties of the femur of the polar bear Ursus maritimus. J Zool **222:**49–58.
43. Carrier D, Leon LR 1990 Skeletal growth and function in the California gull (*Larus californicus*). J Zool **222:**375–389.
44. Martin RB, Boardman DL 1993 The effects of collagen fiber orientation, porosity, density, and mineralization on bovine cortical bone bending properties. J Biomech **26:**1047–1054.
45. Portigliatti Barbos M, Bianco P, Ascenzi A, Boyde A 1984 Collagen orientation in compact bone: II. Distribution of lamellae in the whole of the human femoral shaft with reference to its mechanical properties. Metab Bone Dis Relat Res **5:**309–315.
46. Skedros JG, Sybrowsky CL, Parry TR, Bloebaum RD 2003 Regional differences in cortical bone organization and microdamage prevalence in Rocky Mountain mule deer. Anat Rec **274A:**837–850.
47. Skedros JG, Hunt KJ 2004 Does the degree of laminarity correlate with site-specific differences in collagen fibre orientation in primary bone? An evaluation in the turkey ulna diaphysis. J Anat **205:**121–134.
48. Jepsen KJ, Davy DT, Akkus O 2001 Observations of damage in bone. In: Cowin SC (ed.) Bone Mechanics Handbook, 2nd ed. CRC Press, Boca Raton, FL, USA, pp. 17.1–17.18.
49. Currey JD, Brear K 1992 Fractal analysis of compact bone and antler fracture surfaces. Biomimetics **1:**103–118.
50. Ruff CB 1984 Allometry between length and cross-sectional dimensions of the femur and tibia in Homo sapiens sapiens. Am J Phys Anthropol **65:**347–358.
51. Lanyon LE, Hampson WG, Goodship AE, Shah JS 1975 Bone deformation recorded in vivo from strain gauges attached to the human tibial shaft. Acta Orthop Scand **46:**256–268.
52. Burr DB, Milgrom C, Fyhrie D, Forwood M, Nyska M, Finestone A, Hoshaw S, Saiag E, Simkin A 1996 In vivo measurement of human tibial strains during vigorous activity. Bone **18:**405–410.
53. Boyce TM, Fyhrie DP, Glotkowski MC, Radin EL, Schaffler MB 1998 Damage type and strain mode associations in human compact bone bending fatigue. J Orthop Res **16:**322–329.
54. Schaffler MB, Burr DB 1988 Stiffness of compact bone: Effects of porosity and density. J Biomech **21:**13–16.
55. Milgrom C, Finestone A, Novack V, Pereg D, Goldich Y, Kreiss Y, Zimlichman E, Kaufman S, Liebergall M, Burr D 2004 The effect of prophylactic treatment with risedronate on stress fracture incidence among infantry recruits. Bone **35:**418–424.
56. Schaffler MB, Radin EL, Burr DB 1990 Long-term fatigue behavior of compact bone at low strain magnitude and rate. Bone **11:**321–326.

Address reprint requests to:
Karl J Jepsen, PhD
Department of Orthopaedics
Mount Sinai School of Medicine
Box 1188, One Gustave L. Levy Place
New York, NY 10029, USA
E-mail: karl.jepsen@mssm.edu

Received in original form November 12, 2004; revised form March 16, 2005; accepted March 28, 2005.

JOURNAL OF BONE AND MINERAL RESEARCH
Volume 20, Number 11, 2005
Published online on July 11, 2005; doi: 10.1359/JBMR.050707

Genetic Variation in Bone Growth Patterns Defines Adult Mouse Bone Fragility

Christopher Price,[1] Brad C Herman,[1] Thomas Lufkin,[2] Haviva M Goldman,[3] and Karl J Jepsen[1]

ABSTRACT: Femoral morphology and composition were determined for three inbred mouse strains between ages E18.5 and 1 year. Genotype-specific variation in postnatal, pubertal, and postpubertal growth patterns and mineral accrual explained differences in adult bone trait combinations and thus bone fragility.

Introduction: Fracture risk is strongly regulated by genetic factors. However, this regulation is generally considered complex and polygenic. Therefore, the development of effective genetic-based diagnostic and treatment tools hinges on understanding how multiple genes and multiple cell types interact to create mechanically functional structures. The goal of this study was to connect variability in whole bone mechanical function, including measures of fragility, to variability in the biological processes underlying skeletal development. We accomplished this by testing for variation in bone morphology and composition among three inbred mouse strains from E18.5 to 1 year of age.
Materials and Methods: Mid-diaphyseal cross-sectional areas, diameters, moments of inertia, and ash content were determined for three strains of mice with widely differing adult whole bone femoral mechanical properties (A/J, C57BL/6J, and C3H/HeJ) at E18.5 and postnatal days 1, 7, 14, 28, 56, 112, 182, and 365 (n = 5–15 mice/strain/age).
Results: Significant differences in the magnitude and rate of change in morphological and compositional bone traits were observed among the three strains at each phase of growth, including prenatal, postnatal, pubertal, and adult ages. These genotype-specific variations in growth patterns mathematically determined how variation in adult bone trait combinations and mechanical properties arose. Furthermore, six bone traits were identified that characterize phenotypic variability in femoral growth. These include (1) bone size and shape at postnatal day 1, (2) periosteal and (3) endosteal expansion during early growth, (4) periosteal expansion and (5) endosteal contraction in later growth, and (6) ash content. These results show that genetic variability in adult bone traits arises from variation in biological processes at each phase of growth.
Conclusions: Inbred mice achieve different combinations of adult bone traits through genotype-specific regulation of bone surface activity, growth patterns, and whole bone mineral accrual throughout femoral development. This study provides a systematic approach, which can be applied to the human skeleton, to uncover genetic control mechanisms influencing bone fragility.
J Bone Miner Res 2005;20:1983–1991. Published online on July 11, 2005; doi: 10.1359/JBMR.050707

Key words: genetics, inbred mice, growth and development, bone biomechanics, bone fragility, morphology, ash content

INTRODUCTION

Genetic factors are generally acknowledged to play an important role in the determination of skeletal fragility. Clinically, genetic variability in BMD,[1] bone quality,[2] adult bone morphology,[3] and the kinetics of bone loss[4,5] all contribute to the variation in fracture risk.[6] Therefore, genetic-based screening tools that identify an individual's skeletal growth potential and/or potential for bone loss could be used for the early diagnosis of osteoporotic fracture risk and for tailored treatment regimens thereafter.[7] However, these genetic factors are not completely understood. Additionally, the processes of bone growth and bone loss are genetically complex, such that the modeling and remodeling of complex structures involves the coordinated expression of many genes by multiple cell types (osteoblasts, osteoclasts, and osteocytes).[7] Therefore, a primary challenge for developing effective genetic-based diagnostic tools for fracture risk will be to understand how multiple genes, in multiple cell types, interact throughout life to create and maintain structures that are mechanically and biologically functional.[8]

To study the functional connections between genotype and skeletal fragility, we adopted a top-down approach that

The authors have no conflict of interest.

[1]Leni & Peter W. May Department of Orthopaedics, Mount Sinai School of Medicine, New York, New York, USA; [2]Stem Cell and Developmental Biology, Genome Institute of Singapore, Singapore; [3]Department of Neurobiology and Anatomy, Drexel University College of Medicine, Philadelphia, Pennsylvania, USA.

reveals the functional connections between genotype and skeletal fragility.[9] Our approach uses long bones from inbred mouse strains to relate genetic variability in whole bone mechanical properties to the underlying biological processes regulating bone growth and loss in a systematic and hierarchical manner. Previous research using inbred mice has shown genotype-specific variability in skeletal morphology,[10–12] BMD,[13] mechanical properties,[14,15] bone formation rates,[16,17] and responsiveness to mechanical stimulation.[18,19] Previously, we showed that individual inbred mouse strains exhibited a particular combination of cortical area (Ct.Ar), polar moment of inertia (J_o), and mineral content (ash content) that together explained 66–88% of the genetic variability in adult whole bone mechanical properties.[9] These results indicated that the combination of transverse bone size, shape, and material quality was responsible for the particular repertoire of stiffness, strength, and toughness that characterized each strain. The next step in our systematic approach was to determine how genetic variability in these three physical bone traits (Ct.Ar, J_o, and ash content) arises during the growth process.

Bone traits are influenced by both genetic and environmental factors during growth, and specific combinations of bone traits are established to satisfy the mechanical demands associated with weight bearing.[20] Long bone diaphyses are hollow cylinders whose size and shape can be mathematically determined by the relative amounts of bone apposition and resorption on the periosteal and endosteal surfaces.[21–24] We hypothesize that genetic variability in the rates of periosteal and endosteal expansion throughout life (i.e., growth patterns) defines genotype-specific combinations of adult bone traits. To test this hypothesis, we compared changes in femoral morphology (Ct.Ar and J_o) and composition (ash content) across development (from embryonic day 18.5 [E18.5] to 1 year). Transverse growth was studied because these traits contribute predominantly to the resistance of in vivo loads.[25] Three genetically distinct inbred mouse strains, A/J (A), C57BL/6J (B6), and C3H/HeJ (C3H), with widely differing adult bone trait magnitudes, were examined to better understand the expansive growth of bone surfaces and how this growth leads to unique combinations of adult morphological (Ct.Ar, Tt.Ar, Ma.Ar, and J_o) and compositional (ash content) trait values.[9] We show that variability in skeletal growth patterns reveals the biological and genetic control mechanisms that define adult physical bone traits and, consequently, bone fragility.

MATERIALS AND METHODS

Animals

Female (n = 20/strain) and male (n = 10/strain) A/J (A), C57BL/6J (B6), and C3H/HeJ (C3H) mice were purchased from Jackson Laboratory (Bar Harbor, ME, USA) at 6–8 weeks of age and used to establish breeding colonies. Mice were fed a standard mouse chow (Purina Laboratory Chow 5001; Purina Mills) and water ad libitum and kept on a 12-h light:dark cycle. Matings were monitored, and after 4 weeks of weaning, the offspring were separated by sex and housed with four to five mice per cage. Female offspring were killed at selected time-points for analysis: these included E18.5, postnatal day 1, 7, 14, 28, 56, 112, 182, and 365 (Table 1). For the E18.5 age group, pregnant females were identified by the first appearance of a vaginal plug (designated as day E0.5). The pups were extracted 18 days later through caesarian section and killed by decapitation. All mice 1 day of age and older were killed by carbon dioxide asphyxiation and decapitation. The Mount Sinai Institutional Animal Care and Use Committee approved all procedures for the treatment of mice.

Morphological traits

Right femurs were harvested and embedded in polymethylmethacrylate as described previously.[14] Transverse sections of the femoral diaphyses (150 μm in thickness) were obtained using a low-speed diamond-coated wafering saw (Buehler, Lake Bluff, IL, USA) from a site immediately distal to the third trochanter. The sections were affixed to acrylic slides, polished to 1-μm finish, and stained using von Kossa's method.[26] The sections were imaged with a digital camera (Sony Exwave HAD, 3CCD Camera; Sony) attached to a visible light microscope (Zeiss Axioplan2; Zeiss). The pixel resolution of this optical imaging system was 2.1 μm. An advanced image analysis software package (IMAQ Vision Builder 6.0; National Instruments Corp., Austin, TX, USA) was used to quantify the cross-sectional areas (total area [Tt.Ar], cortical area [Ct.Ar], and marrow area [Ma.Ar]), cortical thickness (Ct.Th), and the polar moment of inertia (J_o). Young bones (ages E18.5 through 2 weeks of age) had a predominantly woven appearance with considerable cortical porosity. Therefore, at these time-points, morphometric measurements included all porosities within the cortical shell and were considered apparent traits. Three cross-sections were analyzed per bone, and the values were averaged. To establish rates of surface growth, the time normalized change in Tt.Ar and Ma.Ar during the early phase of growth (1–28 days of age) and the later phase of growth (28–112 days of age) were obtained from the following equations for all strains:

$$\Delta Tt.Ar_{1-28} = [Tt.Ar_{28} - avg(Tt.Ar_1)]/28 \text{ days} \quad (1)$$

$$\Delta Tt.Ar_{28-112} = [Tt.Ar_{112} - avg(Tt.Ar_{28})]/84 \text{ days} \quad (2)$$

$$\Delta Ma.Ar_{1-28} = [Ma.Ar_{28} - avg(Ma.Ar_1)]/28 \text{ days} \quad (3)$$

$$\Delta Ma.Ar_{Ma.ArMax-112} = [Ma.Ar_{112} - avg(Ma.Ar_{Ma.ArMax})]/(112 - Ma.ArMax) \text{ days} \quad (4)$$

The subscript refers to the age(s) over which the rate was determined. Ma.ArMax corresponds to the age at which maximum Ma.Ar was obtained for a given strain. This age was used as the initial time-point to calculate the rate of marrow infilling during later growth. avg($Tt.Ar_i$) and avg($Ma.Ar_i$) refers to the strain average Tt.Ar and Ma.Ar value at time-point i.

Table 1. Body Weight and Morphological Traits for Femoral Diaphyses of Three Inbred Mouse Strains Between Embryonic Day 18.5 (E18.5) and 1 Year of Age

Strain (age)	*N*	*Weight (g)*	*Cortical area (mm^2)*	*Total area (mm^2)*	*Marrow area (mm^2)*	*J_o (mm^4)*	*Average cortical thickness (mm)*
A							
E18.5	5	—	0.11 ± 0.02†	0.16 ± 0.02†,‡	0.05 ± 0.01†,‡	0.004 ± 0.001†	0.10 ± 0.02
1d	15	1.3 ± 0.1	0.13 ± 0.02†	0.30 ± 0.05†	0.17 ± 0.03	0.010 ± 0.004†	0.08 ± 0.01
7d	12	2.8 ± 0.5‡	0.22 ± 0.02	0.50 ± 0.05†,‡	0.28 ± 0.04†,‡	0.028 ± 0.005	0.11 ± 0.01†
14d	8	6.0 ± 0.4	0.23 ± 0.05‡	0.59 ± 0.08†,‡	0.35 ± 0.05†,‡	0.035 ± 0.011†,‡	0.10 ± 0.02†
28d	8	10.8 ± 1.6	0.37 ± 0.03‡	0.82 ± 0.06†,‡	0.45 ± 0.04†,‡	0.076 ± 0.012†,‡	0.13 ± 0.01†
56d	9	16.4 ± 2.3	0.51 ± 0.09‡	0.97 ± 0.10†,‡	0.46 ± 0.03†	0.119 ± 0.027†,‡	0.18 ± 0.03
112d	13	22.9 ± 3.0†	0.74 ± 0.04‡	1.15 ± 0.8†,‡	0.41 ± 0.05†,‡	0.189 ± 0.023†,‡	0.25 ± 0.02†,‡
182d	12	23.2 ± 1.6†,‡	0.79 ± 0.04‡	1.25 ± 0.06†,‡	0.46 ± 0.03†,‡	0.224 ± 0.024†,‡	0.26 ± 0.02†,‡
365d	9	24.7 ± 2.4	0.79 ± 0.06‡	1.28 ± 0.11†,‡	0.49 ± 0.07†	0.228 ± 0.037†,‡	0.25 ± 0.02‡
B6							
E18.5	10	—	0.17 ± 0.04*,‡	0.33 ± 0.04*,‡	0.16 ± 0.04*,‡	0.014 ± 0.004*,‡	0.10 ± 0.03
1d	15	1.3 ± 0.1	0.16 ± 0.03*	0.35 ± 0.03*	0.19 ± 0.04	0.014 ± 0.003*	0.09 ± 0.02
7d	12	3.1 ± 0.3‡	0.19 ± 0.05	0.61 ± 0.05*	0.41 ± 0.05*,‡	0.032 ± 0.008	0.08 ± 0.02*
14d	12	6.4 ± 0.5‡	0.24 ± 0.04‡	0.90 ± 0.08*,‡	0.66 ± 0.06*,‡	0.061 ± 0.012*	0.08 ± 0.01*,‡
28d	6	10.9 ± 1.0	0.39 ± 0.05	1.24 ± 0.09*,‡	0.85 ± 0.06*,‡	0.133 ± 0.023*,‡	0.11 ± 0.01*,‡
56d	11	16.8 ± 0.8	0.57 ± 0.03‡	1.47 ± 0.07*,‡	0.90 ± 0.05*,‡	0.226 ± 0.022*,‡	0.16 ± 0.01‡
112d	10	20.9 ± 0.6*	0.75 ± 0.03‡	1.55 ± 0.06*,‡	0.80 ± 0.04*,‡	0.297 ± 0.026*	0.21 ± 0.03*,‡
182d	9	21.7 ± 0.9*	0.76 ± 0.05‡	1.48 ± 0.09*,‡	0.72 ± 0.06*,‡	0.283 ± 0.029*	0.20 ± 0.04*,‡
365d	10	25.2 ± 1.8	0.82 ± 0.06‡	1.82 ± 0.10*	1.00 ± 0.07*,‡	0.387 ± 0.044*	0.20 ± 0.02‡
C3H							
E18.5	8	—	0.13 ± 0.01†	0.24 ± 0.03*,†	0.11 ± 0.02*,†	0.007 ± 0.001†	0.10 ± 0.01
1d	15	1.4 ± 0.1	0.15 ± 0.03	0.32 ± 0.03	0.16 ± 0.02	0.012 ± 0.002	0.09 ± 0.02
7d	9	4.4 ± 0.5*,†	0.23 ± 0.06	0.56 ± 0.07*	0.33 ± 0.04*,†	0.032 ± 0.010	0.10 ± 0.02
14d	10	5.7 ± 0.4†	0.31 ± 0.03*,†	0.77 ± 0.11*,†	0.46 ± 0.10*,†	0.059 ± 0.015*	0.12 ± 0.01†
28d	8	10.4 ± 1.5	0.43 ± 0.05*	0.97 ± 0.7*,†	0.54 ± 0.04*,†	0.107 ± 0.017*,†	0.14 ± 0.01†
56d	10	15.6 ± 2.2	0.67 ± 0.07*,†	1.11 ± 0.09*,†	0.44 ± 0.04†	0.174 ± 0.029*,†	0.21 ± 0.04†
112d	11	22.4 ± 1.3	1.08 ± 0.04*,†	1.41 ± 0.06*,†	0.34 ± 0.03*,†	0.310 ± 0.025*	0.34 ± 0.01*,†
182d	9	20.9 ± 0.9*	1.08 ± 0.05*,†	1.35 ± 0.05*,†	0.26 ± 0.04*,†	0.285 ± 0.024*	0.37 ± 0.03*,†
365d	7	23.7 ± 1.8	1.29 ± 0.17*,†	1.71 ± 0.23†	0.42 ± 0.10†	0.448 ± 0.115*	0.35 ± 0.04*,†

* Significantly different from A, ANOVA $p < 0.05$.
† Significantly different from B6, ANOVA $p < 0.05$.
‡ Significantly different from C3H, ANOVA $p < 0.05$.

Compositional traits

Ash content was assessed for the left femurs of all mice 2 weeks of age and older. These femurs had previously been loaded to failure in four-point bending (data not included). The diaphyseal pieces were retrieved and cleaned of all soft tissues under a stereomicroscope. The hydrated, dried, and ashed weights were determined as described previously.[9] Water content was defined as the hydrated weight minus dried weight and expressed as a percentage of hydrated weight. Ash content was determined as the ash weight normalized for hydrated weight.

Statistics

All results are expressed as mean ± SD. Differences in trait values among the three genotypes at each time-point were determined with a one-way ANOVA and a Tukey's posthoc test. A p value less than 0.05 was considered significant (GraphPad Software, San Diego, CA, USA).

RESULTS

Overall changes in femoral diaphyseal structure

All three strains underwent qualitatively similar changes in bone architecture, size, and shape of the mid-diaphyseal cortex as a function of age (Fig. 1). For example, each strain exhibited an entirely woven or porous tissue microstructure at E18.5. However, by 14 days of age, the woven tissue was located only in the posterior-lateral quadrant, and by 28 days of age, the entire mid-diaphysis exhibited a solid, compact, lamellar tissue structure. However, despite similar overall growth patterns, significant variation in bone size, shape, and composition were observed among the strains throughout growth (Table 1).

Prenatal bone growth

Significant differences in total area (Tt.Ar), cortical area (Ct.Ar), and polar moment of inertia (J_o) were observed as early as E18.5 (Fig. 2A; ANOVA, $p < 0.05$). B6 mice showed the largest Ct.Ar, Tt.Ar, and J_o, whereas A mice showed the smallest. C3H mice more closely resembled A mice at E18.5. Between E18.5 and 1 day of age none of the morphological traits changed in B6 mice. In contrast, A and C3H mice showed increases in all three traits, so that by 1 day of age only A mice showed significantly smaller Tt.Ar, Ct.Ar, and J_o values compared with B6 (Fig. 2B; $p < 0.05$).

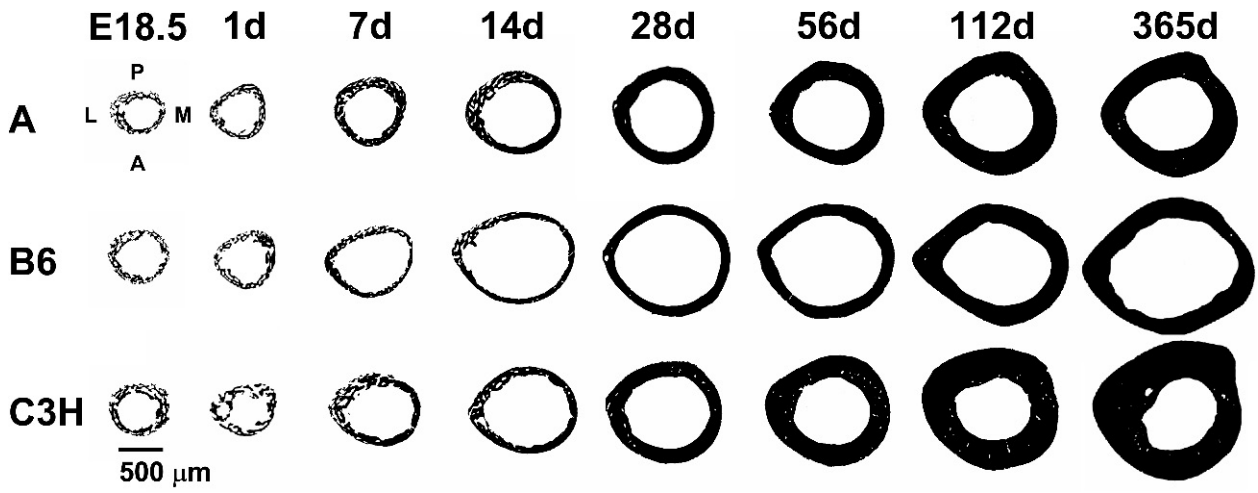

FIG. 1. Variation in femoral cross-sectional morphology across development for female A, B6, and C3H mice. Sections represent equivalent locations within the femoral diaphysis taken immediately distal to the third trochanter. Note change from a porous, woven structure to a compact, lamellar structure between P1 and P28 days of age. Scale bar shown applies to all images.

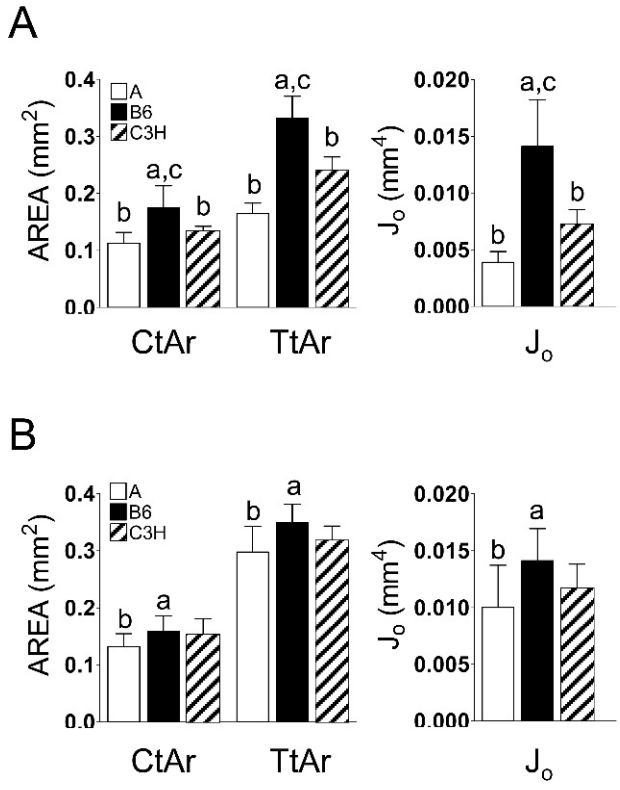

FIG. 2. Variation in femoral cortical area (Ct.Ar), total area (Tt.Ar), and polar moment of inertia (J_o) among A, B6, and C3H mice at (A) embryonic day 18.5 (E18.5) and (B) postnatal day 1. a, b, and c indicates a significant difference from A, B6, and C3H mice, respectively (ANOVA, $p < 0.05$).

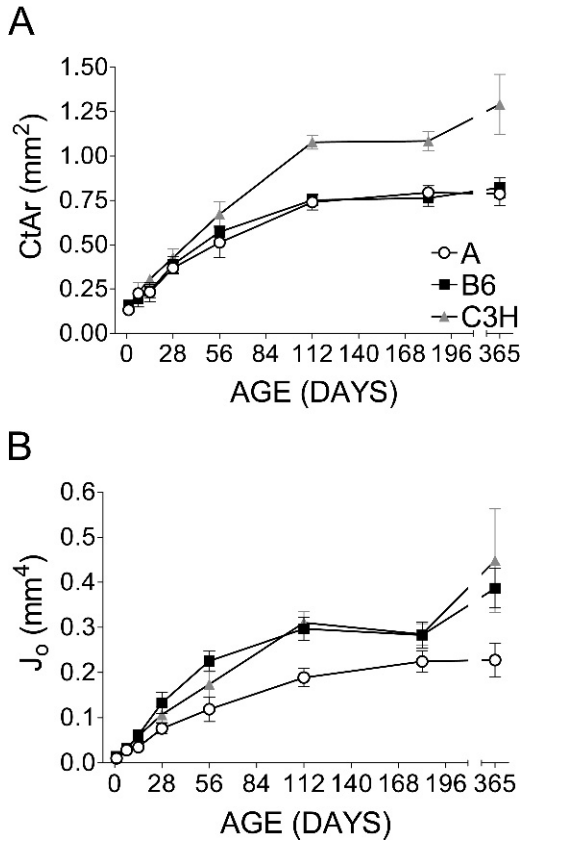

FIG. 3. Variation in (A) cortical area (Ct.Ar), (B) polar moment of inertia (J_o), and (C) ash content across development for A, B6, and C3H femurs. Significant differences among strains in Ct.Ar, J_o, and ash content are indicated in Table 1.

Postnatal changes in Ct.Ar and J_o

After birth, Ct.Ar and J_o increased nonlinearly to 112 days of age (Figs. 3A and 3B). Significant differences in Ct.Ar and J_o values were observed among the strains throughout development (Table 1); however, these differences became more prominent at 56 days of age. For Ct.Ar, A and B6 mice showed similar values beyond 7 days of age, whereas C3H mice showed larger Ct.Ar than both A and

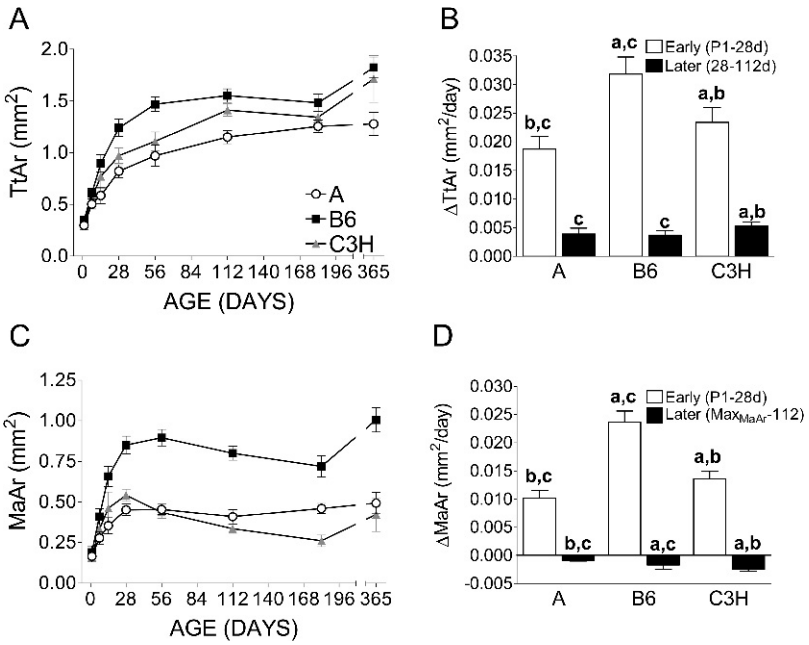

FIG. 4. Variation in femoral total area (Tt.Ar) and marrow area (Ma.Ar) among A, B6, and C3H female mouse strains. (A) Changes in total area across development. (B) Rate of change in total area during early growth (P1–P28 days of age) and later growth (28–112 days of age). (C) Changes in marrow area across development. (D) Rate of change in marrow area during early growth (P1–P28 days of age) and growth after maximum marrow area was achieved ($Ma.Ar_{Max}$–112 days of age). Significant differences among strains in Tt.Ar and Ma.Ar are indicated in Table 1. a, b, and c indicates a significant difference from A, B6, and C3H mice, respectively, at the indicated timepoint.

B6 after 14 days of age (ANOVA, $p < 0.05$). For J_o, B6 and C3H mice showed similar values beyond 56 days of age, whereas A mice showed smaller values compared with B6 and C3H beyond 14 days of age ($p < 0.05$). These differences in physical bone traits were accompanied by nearly identical age-related increases in body weight among all strains (Table 1).

Postnatal expansion of the periosteal surface

Tt.Ar increased nonuniformly with age in a genotype-dependent manner (Fig. 4A). Each strain achieved 80–90% of adult Tt.Ar and periosteal diameter by 28 days of age. In contrast, all three strains achieved only 40–50% of adult weight, Ct.Ar, and J_o by this age. These data indicated that the periosteum expanded rapidly for all strains early in life. However, the rate of expansion at the periosteum (i.e., increase in Tt.Ar per day) during early growth, and the size of Tt.Ar at 28 days of age differed significantly among the strains (B6 > C3H > A; ANOVA, $p < 0.05$; Fig. 4B; Table 1). Between 28 and 112 days of age, the average rate of increase in Tt.Ar was reduced by ~80% compared with the rates observed between P1 and P28 days of age. During the later phase of growth (28–112 days), the rate of Tt.Ar expansion was greatest in C3H mice, whereas A and B6 mice showed similarly lower rates of expansion ($p < 0.05$). Age-related changes in periosteal diameter mirrored the changes in Tt.Ar, as expected (data not shown).

Postnatal expansion of the endosteal surface

Like Tt.Ar, marrow area (Ma.Ar) also changed nonuniformly with age and in a genotype-dependent manner (Fig. 4C). All mouse strains exhibited similar Ma.Ar values at birth and exhibited rapid postnatal marrow expansion between P1 and P28 days of age. During this early growth phase, B6 femurs exhibited the greatest rate of endosteal expansion (resorption), followed by C3H mice, and then A mice, resulting in significant differences in Ma.Ar size at 28 days of age (A < B6 < C3H; ANOVA, $p < 0.05$; Fig. 4D). Maximum Ma.Ar values were achieved for A and C3H mice at ~28 days of age, whereas this did not occur until 56 days of age for B6 mice. After reaching maximal Ma.Ar values, all strains exhibited decreases in Ma.Ar, indicating that the endosteal surface underwent a reversal in biological activity from net resorption to net apposition (i.e., infilling). During the period between the time of maximal Ma.Ar and 112 days of age, the three strains of mice showed significantly different rates of endosteal contraction (apposition; A < B6 < C3H; $p < 0.05$). As a result, adult Ma.Ar at 112 days of age was largest in B6 mice because of the early rapid expansion of the marrow cavity and smallest in C3H mice because of its slower marrow excavation and larger fractional infilling. Age-related changes in endosteal diameter were similar to those observed for Ma.Ar, as expected (data not shown).

Age-related changes in cortical thickness

Changes in cortical thickness (Ct.Th) reflected the relative rate of expansion of the periosteal and endosteal surfaces. The average cortical thickness increased nonlinearly between birth and 1 year of age in all three strains (Fig. 5). Between E18.5 and 7 days of age, the average cortical thickness did not change significantly for any of the strains indicating that expansion of the marrow cavity kept pace with expansion of the periosteum. However, beyond 14 days of age, cortical thickness increased linearly until peak values were obtained at 112 days of age. After 14 days of age, C3H femurs exhibited cortices with the largest average thickness, A femurs exhibited intermediate cortical thickness, and B6 the smallest (ANOVA, $p < 0.05$).

Postnatal changes in ash content

In all three strains, ash content increased with age to 112 days (Fig. 6). Genotype-specific variation in ash content

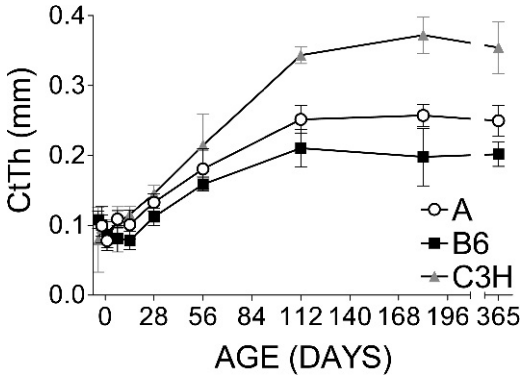

FIG. 5. Variation in femoral cortical thickness (Ct.Th) among A, B6, and C3H mice across development. Significant differences in Ct.Th among strains are indicated in Table 1.

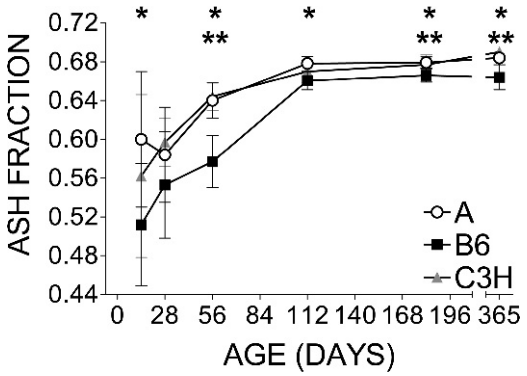

FIG. 6. Variation in femoral ash content across development for A, B6, and C3H femurs. *B6 < A (ANOVA; $p < 0.05$); **B6 < C3H (ANOVA; $p < 0.05$).

was observed at the earliest time-point assayed (2 weeks of age), and these relationships persisted throughout the remainder of the study.

DISCUSSION

This study showed that genetic variability in inbred mouse adult bone traits (Ct.Ar, J_o, and ash content) results directly from genotype-specific differences in periosteal and endosteal expansion and whole bone mineral accrual, as hypothesized. Previous studies comparing B6 and C3H mouse growth suggested that genetic variation in adult bone mass could be explained by prepubertal and pubertal growth patterns[27] and by different rates of bone formation during adolescent growth.[16] Additional studies examined B6 skeletal development alone.[28,29] However, these studies did not include prenatal and immediate postnatal growth (<7 days). Therefore, it remained unclear how in utero growth, early bone cell (osteoblast and osteoclast) activities, and peripubertal/adolescent growth contributed to genetic variability in adult trait magnitudes. By looking across growth, including several time-points not previously studied, we were able to connect early and later bone development. Thus, this work filled in gaps from previous studies and provided new insight into the genetic regulation of adult bone traits. Furthermore, we studied both the spatial distribution of bone (J_o) and matrix mineralization (ash content). Previous work from our laboratory has shown that these traits in combination with tissue amount (Ct.Ar) are important in the determination of whole bone strength and brittleness, respectively.[9] Last, we included a third strain (A), which was previously shown to have a small adult bone morphology and high adult ash content,[9,14] to further generalize how genetic background influences adult bone traits.

Our examination of bone morphology from E18.5 to 365 days of age revealed that A, B6, and C3H inbred mouse strains showed qualitatively similar transverse femoral growth patterns. The early rapid expansion of the periosteal and endosteal surfaces followed by marrow infilling observed for the mouse was consistent with that observed for human long bones.[21] As such, studying the genetic regulatory pathways controlling murine long bone growth and the attainment of peak bone properties should prove valuable in understanding similar processes in the human skeleton.

The attainment of a particular combination of Ct.Ar and J_o in adult inbred mice can be explained in mathematical terms based on variability in the relative expansion of the periosteal and endosteal surfaces during growth when the femoral diaphysis is modeled as a simple hollow cylinder.[20–22] Because Ct.Ar and J_o are related to periosteal and endosteal diameters differently,

$$\text{Ct.Ar} = \text{Tt.Ar} - \text{Ma.Ar} \propto \text{Dia}_{\text{Peri}}^2 - \text{Dia}_{\text{Endo}}^2 \quad (5)$$

$$J_o \propto \text{Tt.Ar}^2 - \text{Ma.Ar}^2 \propto \text{Dia}_{\text{Peri}}^4 - \text{Dia}_{\text{Endo}}^4 \quad (6)$$

cylinders of different diameters will necessarily have different combinations of Ct.Ar and J_o values. Thus, variability in adult Ct.Ar and J_o arise during growth necessarily because differences in the relative expansion of the periosteal and endosteal surface (i.e., growth patterns) lead to different periosteal and endosteal diameters.

We found that the unique pattern of periosteal and endosteal growth exhibited throughout life by each genotype could indeed explain, in mathematical terms, how variability in adult morphological trait combinations (Ct.Ar and J_o) arises. For B6 mice, the large J_o and small Ct.Ar observed in adulthood resulted primarily from a large periosteal and endosteal expansion during early growth (before puberty). For C3H mice, an intermediate rate of periosteal and endosteal expansion during early growth (compared with A and B6) and a significantly greater periosteal expansion and marrow infilling after puberty led to the large Ct.Ar and J_o values of adult C3H mice. As a result, Ct.Ar and J_o increased at a faster rate in C3H mice and led to a higher Ct.Ar relative to J_o because a larger proportion of new bone was added, in a less mechanically efficient manner, to the endosteum. It is noteworthy that B6 and C3H mice achieved similar adult J_o values. However, this occurred through very different growth patterns and, presumably, different biological control mechanisms. For A mice, the small adult Ct.Ar and J_o were a result of having the smallest periosteal and endosteal expansion both before and after

puberty. Interestingly, A and B6 mice achieved similar adult Ct.Ar values, but this occurred through very different growth patterns, suggesting that A and B6 mice achieve similar adult Ct.Ar through different biological control mechanisms. Together these results show that inbred mice build morphologically distinct femurs by regulating bone surface activity in a genotype-specific manner.

From these data, we identified six bone traits that helped characterize the variability in transverse femoral development among three strains of inbred mice and that provided additional insight into the biological control mechanisms underlying variability in adult bone traits. The six traits included (1) the initial size of the bone at 1 day of age, (2) periosteal expansion during the early (prepubertal), rapid growth phase, (3) endosteal expansion during the early growth phase, (4) periosteal expansion during the later (peri- to postpubertal) growth phase, (5) marrow infilling during the later growth phase, and (6) ash content (material composition) throughout growth. Interstrain variability in the first five indices reflects differences in bone cell activity during different growth phases, and the last index reflects variation in the tissue mineralization process. Together, these bone traits represent phenotypic indices that will be useful for identifying the biological (and genetic) mechanisms that influence adult whole bone mechanical properties.

Variability in bone size and shape (Ct.Ar, J_o, and TAr) at E18.5 and 1 day of age show that these inbred mice begin postnatal skeletal development with different initial morphologies. These results suggest that bone growth and adult bone mass might be related to allelic variability in the factors involved in in utero development. Differences in tissue patterning and condensation have been observed in the cranio-facial development of B6 and C3H mice,[30] and similar variability in tissue patterning and condensation, cartilage formation, or initial bone formation could influence long bone morphology at birth. Research in humans has identified correlations between in utero growth, postnatal growth, and adult bone mass that support the idea that pre- and postnatal growth influence adult skeletal properties.[31–33] Additional studies in mice may be useful in establishing the relationship between prenatal morphology and growth and adult bone trait values.

Investigation of early growth (1–28 days of age) revealed that prepubertal growth played a critical role in defining adult trait values. Strain specific differences in adult external size were established during early growth, suggesting that variation in Tt.Ar, bone width, and maximal Ma.Ar are likely the result of allelic variations influencing the processes controlling rapid surface expansion before puberty. Measures of adult bone morphology, which have been correlated with fracture risk,[3,34] are also largely determined before puberty in humans.[21] Therefore, the mouse may provide a useful model for studying how fracture risk is associated with the biology of early bone growth and the establishment of external size.

Variability in ash content was also established at the earliest time-point studied (2 weeks of age) and was consistent with the variability observed in adulthood. This suggested that differences in mineralization and material composition among the strains might be observed even earlier in life, possibly before birth, or within the first few days of postnatal growth. We previously showed that a 4.0% variation in ash content among inbred strains was correlated with a ~3.4- and ~1.9-fold variation in whole bone ductility and toughness, respectively.[14] Therefore, the consistently lower B6 femoral ash content, compared with A and C3H mice, implied that B6 femurs were constructed of bone tissue with a lower material stiffness but greater ductility[35] throughout life. Together, these results suggest that different strains of inbred mice might harbor allelic variations in the genetic factors inherent to or governing mineral accrual.

The rate and extent of periosteal and endosteal expansion during early growth appeared to be well matched to ash content values, suggesting that material composition may be functionally coupled to bone growth patterns. B6 mice, with the most rapid prepubertal surface expansions and largest Tt.Ar and J_o values at 28 days of age, showed small ash values. In contrast, the slower expanding bones of A and C3H mice showed larger ash values. From a mechanical basis, these results are not entirely surprising because the addition of an equivalent amount of tissue on the outer surface of a large bone will result in a greater increase in J_o, and therefore bone stiffness,[29,35] compared with a similar addition on a smaller bone. Thus, the rapid expansion of the periosteum and endosteum in B6 mice established a more efficient growth pattern compared with A and C3H mice. This greater structural efficiency would substantially increase whole bone stiffness and presumably afford B6 mice the ability to reach a mechanically functional end state with material of reduced ash content and thus reduced tissue level stiffness.

The variability in femoral growth patterns observed after the onset of puberty were entirely consistent with previously reported data.[16,27,29] Furthermore, our comparison of early and later growth suggests that female C3H mice might harbor allelic variations that significantly alter their growth patterns after puberty and predispose them to drastically increased bone growth in association with sexual maturation. Additional studies are required to test if pubertal maturation and sex hormones differentially affect the biological processes of skeletal growth and contribute to the variability in adult bone traits among these strains.

Significant variation in the aging of the inbred mouse skeleton was also observed. A mice showed no changes in Tt.Ar and Ma.Ar values between 182 and 365 days of age, suggesting little periosteal expansion and endosteal expansion during this time, whereas B6 and C3H mice showed large increases in Tt.Ar and Ma.Ar. The age-related expansion of B6 and C3H femurs is similar to that observed for the human skeleton.[21,36] These results suggest that the biological processes associated with skeletal aging vary with genetic background.

Although female A, B6, and C3H mice exhibited a wide range of skeletal phenotypes, further studies are warranted to test how growth patterns vary among other strains of mice, how growth patterns vary between male and females,[21,23,24] and how each phase of growth is related to biomechanical properties. In a standard cylindrical model of growth, measures of Tt.Ar and Ma.Ar are sufficient to

describe how a single species of bone cells (osteoblasts or osteoclast) influence surface changes. However, the transverse growth of the femoral mid-diaphysis occurs through both surface expansion and cortical drift.[37,38] In regions of long bones exhibiting drift, both apposition and resorption occur at different locations along each surface; therefore, the relative contribution of osteoblasts and osteoclasts working on both the periosteum and endosteum must be considered in the analysis of Tt.Ar and Ma.Ar, respectively.

From this study, we conclude that different strains of inbred mice build distinct, yet mechanically functional, femurs by regulating bone surface activity and mineral accrual in a genotype-specific manner. These genotype-specific growth patterns led directly to particular combinations of adult bone traits, and thus, specific repertoires of whole bone mechanical properties. By looking across all ages of growth, from prenatal development to adulthood, we identified six bone traits that can be used to explain, in a systematic manner, the differences in femoral growth patterns among inbred mice. This characterization of femoral growth for A, B6, and C3H mice throughout life revealed how and when specific combinations of adult bone traits arise in genetically distinct animals. Thus, the inbred mouse provides a valuable model to determine how genetic background influences the biological processes involved in establishing variability in adult bone traits, and thus, whole bone mechanical properties.

ACKNOWLEDGMENTS

The authors thank the National Institutes of Health (AR44927), and the Department of Defense (DAMD 17-01-1-0806) for support.

REFERENCES

1. Fox KM, Cummings SR, Powell-Threets K, Stone K 1998 Family history and risk of osteoporotic fracture. Study of Osteoporotic Fractures Research Group. Osteoporos Int **8:**557–562.
2. Howard GM, Nguyen TV, Harris M, Kelly PJ, Eisman JA 1998 Genetic and environmental contributions to the association between quantitative ultrasound and bone mineral density measurements: A twin study. J Bone Miner Res **13:**1318–1327.
3. Nelson DA, Barondess DA, Hendrix SL, Beck TJ 2000 Cross-sectional geometry, bone strength, and bone mass in the proximal femur in black and white postmenopausal women. J Bone Miner Res **15:**1992–1997.
4. Kelly PJ, Hopper JL, Macaskill GT, Pocock NA, Sambrook PN, Eisman JA 1991 Genetic factors in bone turnover. J Clin Endocrinol Metab **72:**808–813.
5. Kelly PJ, Nguyen T, Hopper J, Pocock N, Sambrook P, Eisman J 1993 Changes in axial bone density with age: A twin study. J Bone Miner Res **8:**11–17.
6. Bouxsein ML 2003 Bone quality: Where do we go from here? Osteoporos Int **14**(Suppl 5)**:**118–127.
7. Huang QY, Recker RR, Deng HW 2003 Searching for osteoporosis genes in the post-genome era: Progress and challenges. Osteoporos Int **14:**701–715.
8. Nadeau JH, Burrage LC, Restivo J, Pao YH, Churchill G, Hoit BD 2003 Pleiotropy, homeostasis, and functional networks based on assays of cardiovascular traits in genetically randomized populations. Genome Res **13:**2082–2091.
9. Jepsen KJ, Akkus OJ, Majeska RJ, Nadeau JH 2003 Hierarchical relationship between bone traits and mechanical properties in inbred mice. Mamm Genome **14:**97–104.
10. Stein K 1957 Genetical studies on the skeleton of the mouse XXI. The girdles and the long bones. J Genet **55:**313–324.
11. Lovell D, Johnson F 1983 Quantitative genetic variation in the skeleton of the mouse. Genet Res **42:**169–182.
12. Lovell D, Johnson F, Willis D 1986 Quantitative genetic variation in the skeleton of the mouse: II Description of variation within and between inbred strains. Am J Anat **176:**287–303.
13. Beamer WG, Donahue LR, Rosen CJ, Baylink DJ 1996 Genetic variability in adult bone density among inbred strains of mice. Bone **18:**397–403.
14. Jepsen KJ, Pennington DE, Lee YL, Warman M, Nadeau J 2001 Bone brittleness varies with genetic background in A/J and C57BL/6J inbred mice. J Bone Miner Res **16:**1854–1862.
15. Akhter MP, Fan Z, Rho JY 2004 Bone intrinsic material properties in three inbred mouse strains. Calcif Tissue Int **75:**416–420.
16. Sheng MH, Baylink DJ, Beamer WG, Donahue LR, Rosen CJ, Lau KH, Wergedal JE 1999 Histomorphometric studies show that bone formation and bone mineral apposition rates are greater in C3H/HeJ (high-density) than C57BL/6J (low-density) mice during growth. Bone **25:**421–429.
17. Akhter MP, Iwaniec UT, Covey MA, Cullen DM, Kimmel DB, Recker RR 2000 Genetic variations in bone density, histomorphometry, and strength in mice. Calcif Tissue Int **67:**337–344.
18. Akhter MP, Cullen DM, Pedersen EA, Kimmel DB, Recker RR 1998 Bone response to in vivo mechanical loading in two breeds of mice. Calcif Tissue Int **63:**442–449.
19. Amblard D, Lafage-Proust MH, Laib A, Thomas T, Ruegsegger P, Alexandre C, Vico L 2003 Tail suspension induces bone loss in skeletally mature mice in the C57BL/6J strain but not in the C3H/HeJ strain. J Bone Miner Res **18:**561–569.
20. Sumner DR, Andriacchi TP 1996 Adaptation to differential loading: Comparison of growth-related changes in cross-sectional properties of the human femur and humerus. Bone **19:**121–126.
21. Garn SM 1970 The Earlier Gain and the Later Loss of Cortical Bone, in Nutritional Perspective. Thomas, Springfield, IL, USA.
22. van der Meulen MC, Beaupre GS, Carter DR 1993 Mechanobiologic influences in long bone cross-sectional growth. Bone **14:**635–642.
23. Duan Y, Beck TJ, Wang XF, Seeman E 2003 Structural and biomechanical basis of sexual dimorphism in femoral neck fragility has its origins in growth and aging. J Bone Miner Res **18:**1766–1774.
24. Seeman E 1997 From density to structure: Growing up and growing old on the surfaces of bone. J Bone Miner Res **12:**509–521.
25. Selker F, Carter DR 1989 Scaling of long bone fracture strength with animal mass. J Biomech **22:**1175–1183.
26. Johnson FB 1992 Von Kossa method for minerals. In: Prophet EB (ed.) Laboratory Methods in Histotechnology. American Registry of Pathology, Washington, DC, USA, p. 197.
27. Richman C, Kutilek S, Miyakoshi N, Srivastava AK, Beamer WG, Donahue LR, Rosen CJ, Wergedal JE, Baylink DJ, Mohan S 2001 Postnatal and pubertal skeletal changes contribute predominantly to the differences in peak bone density between C3H/HeJ and C57BL/6J mice. J Bone Miner Res **16:**386–397.
28. Ferguson VL, Ayers RA, Bateman TA, Simske SJ 2003 Bone development and age-related bone loss in male C57BL/6J mice. Bone **33:**387–398.
29. Brodt MD, Ellis CB, Silva MJ 1999 Growing C57Bl/6 mice increase whole bone mechanical properties by increasing geometric and material properties. J Bone Miner Res **14:**2159–2166.
30. Miyake T, Cameron AM, Hall BK 1997 Variability of embryonic development among three inbred strains of mice. Growth Dev Aging **61:**141–155.
31. Gale CR, Martyn CN, Kellingray S, Eastell R, Cooper C 2001 Intrauterine programming of adult body composition. J Clin Endocrinol Metab **86:**267–272.

32. Cooper C, Fall C, Egger P, Hobbs R, Eastell R, Barker D 1997 Growth in infancy and bone mass in later life. Ann Rheum Dis **56:**17–21.
33. Loro ML, Sayre J, Roe TF, Goran MI, Kaufman FR, Gilsanz V 2000 Early identification of children predisposed to low peak bone mass and osteoporosis later in life. J Clin Endocrinol Metab **85:**3908–3918.
34. Giladi M, Milgrom C, Simkin A, Stein M, Kashtan H, Margulies J, Rand N, Chisin R, Steinberg R, Aharonson Z 1987 Stress fractures and tibial bone width. A risk factor. J Bone Joint Surg Br **69:**326–329.
35. Currey JD 2004 Tensile yield in compact bone is determined by strain, post-yield behaviour by mineral content. J Biomech **37:**549–556.
36. Lazenby RA 1990 Continuing periosteal apposition. I: Documentation, hypotheses, and interpretation. Am J Phys Anthropol **82:**451–472.
37. Sontag W 1986 Quantitative measurement of periosteal and cortical-endosteal bone formation and resorption in the midshaft of female rat femur. Bone **7:**55–62.
38. Enlow DH 1962 A study of the post-natal growth and remodeling of bone. Am J Anat **110:**79–101.

Address reprint requests to:
Karl J Jepsen, PhD
Department of Orthopaedics
Mount Sinai School of Medicine
Box 1188, One Gustave L. Levy Place
New York, NY 10029, USA
E-mail: karl.jepsen@mssm.edu

Received in original form May 13, 2005; revised form June 16, 2005; accepted July 5, 2005.